iScience

CellPress
OPEN ACCESS

Article

TORC1 inactivation promotes APC/C-dependent mitotic slippage in yeast and human cells

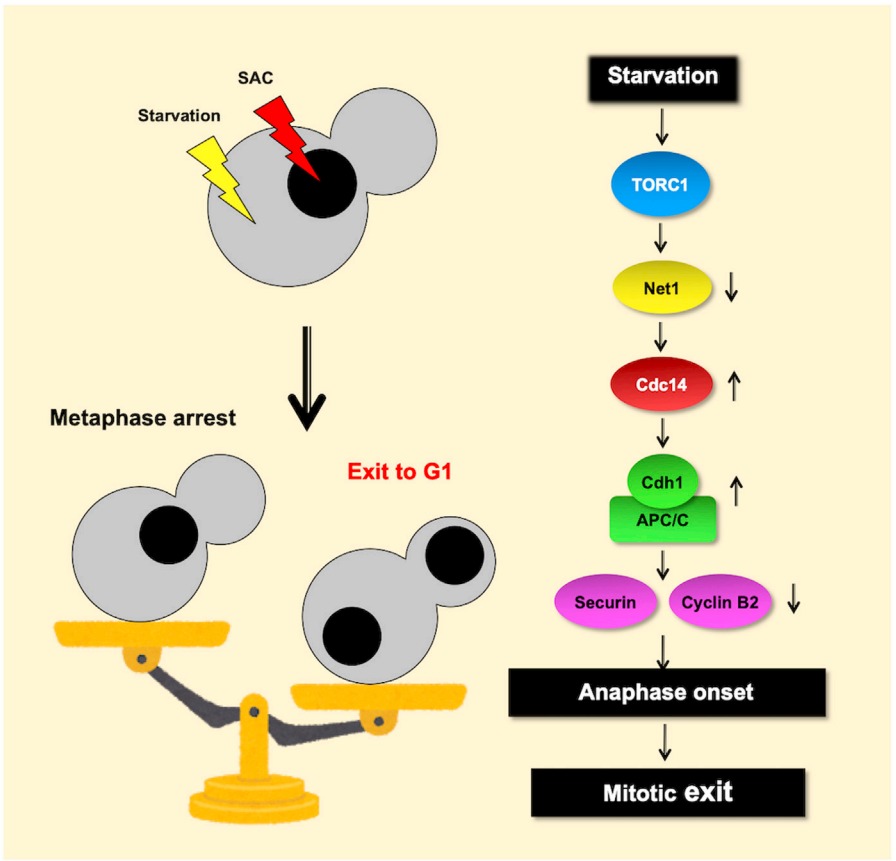

Chihiro Yamada, Aya Morooka, Seira Miyazaki, ..., Kotaro Ohara, Kozo Tanaka, Takashi Ushimaru

ushimaru.takashi@shizuoka.ac.jp

Highlights

Yeast TORC1 inhibition promotes Net1 degradation and Cdc14 release

Yeast TORC1 inhibition invokes mitotic slippage in an APC/C-Cdh1-dependent manner

Human mTORC1 inhibition also elicits mitotic slippage

Yamada et al., iScience *25*, 103675
February 18, 2022
https://doi.org/10.1016/j.isci.2021.103675

iScience

CellPress
OPEN ACCESS

Article

TORC1 inactivation promotes APC/C-dependent mitotic slippage in yeast and human cells

Chihiro Yamada,[1] Aya Morooka,[2] Seira Miyazaki,[2] Masayoshi Nagai,[1,3] Satoru Mase,[1] Kenji Iemura,[3] Most Naoshia Tasnin,[4] Tsuneyuki Takuma,[1] Shotaro Nakamura,[1] Shamsul Morshed,[4,5] Naoki Koike,[4] Md. Golam Mostofa,[4,6] Muhammad Arifur Rahman,[4,7] Tasnuva Sharmin,[4,8] Haruko Katsuta,[1] Kotaro Ohara,[2] Kozo Tanaka,[3] and Takashi Ushimaru[1,2,4,9,*]

SUMMARY

Unsatisfied kinetochore-microtubule attachment activates the spindle assembly checkpoint to inhibit the metaphase-anaphase transition. However, some cells eventually override mitotic arrest by mitotic slippage. Here, we show that inactivation of TORC1 kinase elicits mitotic slippage in budding yeast and human cells. Yeast mitotic slippage was accompanied with aberrant aspects, such as degradation of the nucleolar protein Net1, release of phosphatase Cdc14, and anaphase-promoting complex/cyclosome (APC/C)-Cdh1-dependent degradation of securin and cyclin B in metaphase. This mitotic slippage caused chromosome instability. In human cells, mammalian TORC1 (mTORC1) inactivation also invoked mitotic slippage, indicating that TORC1 inactivation-induced mitotic slippage is conserved from yeast to mammalian cells. However, the invoked mitotic slippage in human cells was not dependent on APC/C-Cdh1. This study revealed an unexpected involvement of TORC1 in mitosis and provides information on undesirable side effects of the use of TORC1 inhibitors as immunosuppressants and anti-tumor drugs.

INTRODUCTION

Accurate chromosome segregation is essential for cell proliferation and genome stability in all organisms. Errors in chromosome segregation result in aneuploidy, which is manifested in genetic disorders and cancer. The spindle assembly checkpoint (SAC) ensures faithful chromosome segregation during cell division (Bharadwaj and Yu, 2004; Musacchio and Salmon, 2007). In the presence of unsatisfied kinetochore-microtubule attachments, the SAC inhibits anaphase onset by inhibition of the ubiquitin ligase (E3) Cdc20-associated anaphase-promoting complex/cyclosome (APC/C). The SAC recruits various checkpoint proteins to unattached kinetochores, and checkpoint proteins Mad2, BubR1 (Mad3 in yeast), and Bub3 bind to and inhibit APC/C-Cdc20 (Kulukian et al., 2009). Once proper kinetochore-microtubule attachments are established, the SAC is deactivated and APC/C-Cdc20 becomes active and mediates degradation of the separase inhibitor securin. Liberated separase cleaves the cohesin subunit Scc1/Mcd1/Rad21, allowing sister chromatid separation (anaphase onset) (Peters et al., 2008).

Microtubule poisons are of clinical importance in the successful treatment of a variety of human cancers, because they activate the SAC and induce mitotic arrest, which eventually leads to apoptotic cell death (Rieder and Maiato, 2004). However, in the course of prolonged treatment with such drugs, some cells escape from mitosis, resulting in aneuploid cells (Minn et al., 1996; Rieder and Maiato, 2004). This phenomenon is called mitotic slippage, and it is responsible for the failure to efficiently block tumor progression. Mitotic slippage depends on progressive degradation of cyclin B, although the SAC is active, indicating that mitotic slippage occurs through the overriding of activated SAC signaling (Brito and Rieder, 2006; Gascoigne and Taylor, 2008). Mitotic exit occurs once cyclin B-Cdk1 activity has decreased below a critical threshold required to maintain a mitotic state (Brito and Rieder, 2006). In addition to cyclin B, other mitotic APC/C substrates, including securin, are also degraded during mitotic slippage. Mitotic slippage occurs in a manner dependent on APC/C (Brito and Rieder, 2006; Gascoigne and Taylor, 2008; Lee et al., 2010). It is likely that mitotic slippage in human cells is mainly driven by APC/C-Cdc20 resulting from incomplete repression of the SAC (Brito and Rieder, 2006; Collin et al., 2013; Dick and Gerlich, 2013; Huang et al., 2009).

[1]Department of Science, Graduate School of Integrated Science and Technology, Shizuoka University, Shizuoka 422-8021, Japan

[2]Department of Biological Science, Faculty of Science, Shizuoka University, 836 Ohya, Suruga-ku, Shizuoka 422-8529, Japan

[3]Department of Molecular Oncology, Institute of Development, Aging and Cancer, Tohoku University, 4-1 Seiryo-machi, Aoba-ku, Sendai, Miyagi 980-8575, Japan

[4]Graduate School of Science and Technology, Shizuoka University, Ohya 836, Suruga-ku, Shizuoka 422-8021, Japan

[5]Present address: Chattogram Veterinary and Animal Sciences University, Khulshi, Chattogram 4225, Bangladesh

[6]Present address: Department of Physiology and Neurobiology, University of Connecticut, Storrs, CT 06269, USA

[7]Present address: Department of Biology, Georgia State University, P.O. Box 4010, Atlanta, GA 30302e4010, USA

[8]Present address: Department of Pharmaceutical Chemistry, Faculty of Pharmacy, University of Dhaka, Dhaka 1000, Bangladesh

[9]Lead contact

*Correspondence: ushimaru.takashi@shizuoka.ac.jp

https://doi.org/10.1016/j.isci.2021.103675

Cdc20 is activated at metaphase-anaphase transition, whereas the Cdc20 homolog Cdh1 is normally activated in late mitosis. In the budding yeast *Saccharomyces cerevisiae*, APC/C-Cdh1 is activated at telophase (Schwab et al., 1997; Visintin et al., 1997). The switch from APC/C-Cdc20 to APC/C-Cdh1 is regulated by multiple mechanisms (Simanis, 2003; Stegmeier and Amon, 2004; Sullivan and Morgan, 2007; Tan et al., 2005). Cyclin B-Cdk1 (Cdc28 in yeast) phosphorylates and inhibits Cdh1 until anaphase, but the cyclin-dependent kinase (CDK)-antagonizing phosphatase Cdc14 dephosphorylates and activates Cdh1 upon telophase onset. Recently, we found that Cdh1 is partially active and mediates securin degradation even in SAC-active metaphase cells of budding yeast (Nagai and Ushimaru, 2014). These results indicated that Cdh1 has a potential to oppose the SAC and promote anaphase transition. Indeed, we reported Cdh1-mediated mitotic slippage: if Cdh1 is further activated in metaphase by loss of Bub2, an inhibitor of the mitotic exit network (MEN) pathway, APC/C-Cdh1 aberrantly mediates securin degradation at metaphase with the SAC active (Toda et al., 2012). However, it is still unknown in what kind of physiological (stress) conditions Cdh1-mediated mitotic slippage is promoted in wild-type strains.

Target of rapamycin complex 1 (TORC1) kinase is a central controller of cell growth and proliferation in response to nutrient availability. TORC1 controls diverse cellular events, including transcription, translation, and autophagy (Loewith and Hall, 2011; Zoncu et al., 2011). Mammalian TORC1 (mTORC1) is crucially involved in diabetes, cancer, and aging (Cornu et al., 2013; Shimobayashi and Hall, 2014; Zoncu et al., 2011). Of note, treatment with rapamycin, a specific TORC1 inhibitor, induces chromosome instability in yeast and mammalian cells (Bonatti et al., 1998; Choi et al., 2000). This indicates that TORC1 is critical for accurate genome transmission, although its molecular mechanism remains elusive. Here we show that nutrient starvation and TORC1 inhibition antagonize CDK and promote Cdh1-mediated mitotic slippage and chromosome instability via an aberrant pathway in yeast cells. Furthermore, mammalian TORC1 (mTORC1) inactivation provoked mitotic slippage in a different manner in human cells. This study uncovered an unconventional conserved role of TORC1 as a regulator of mitotic progression.

RESULTS

TORC1 inactivation overrides SAC-mediated metaphase arrest

Because rapamycin induces chromosome instability (Bonatti et al., 1998; Choi et al., 2000), we suspected that TORC1 inactivation compromises SAC function. Here, we tested this idea using budding yeast. Securin/Pds1 degradation was repressed by the SAC in nocodazole-treated metaphase cells (Figure 1A, -Rap), whereas rapamycin facilitated securin degradation (Figure 1A, +Rap). Furthermore, rapamycin evoked cleavage of Scc1, a kleisin subunit of cohesin, and sister chromatid separation (Figures 1B and 1C and also see Figure 2F, WT). These findings indicated that TORC1 inactivation overrode SAC-mediated metaphase arrest. Because microtubule formation was impaired by nocodazole, rapamycin-induced sister chromatid separation was not remarkable compared with nocodazole removal-induced one, despite Scc1 cleavage in these conditions (see Figure 3C, WT + Rap and WT-Noc).

We assessed whether rapamycin-mediated TORC1 inactivation overcame metaphase arrest in different SAC-active conditions. Cells of the temperature-sensitive *SCC1* mutant *scc1-73* are defective in tension generation between sister kinetochores and arrest in metaphase with the SAC active at restrictive temperatures (Severin et al., 2001). Securin accumulated in *scc1-73* cells at 37°C, but securin degradation was induced by rapamycin treatment (Figure S1A). Overexpression of the SAC kinase Mps1 activates the SAC, leading to metaphase arrest (Hardwick et al., 1996). Rapamycin promoted chromosome segregation in *MPS1* overexpression-mediated metaphase arrest (Figure S1B). Thus, TORC1 inactivation overcame various types of SAC-mediated metaphase arrest.

Nitrogen depletion causes TORC1 inactivation (Loewith and Hall, 2011; Zoncu et al., 2011). Securin degradation was similarly evoked by nitrogen starvation (Figure 1D). Overall, starvation and TORC1 inactivation overrode SAC-mediated metaphase arrest and evoked anaphase onset (Figure 1E).

APC/C-Cdh1 mediates TORC1 inactivation-induced anaphase onset

Securin degradation after rapamycin treatment suggested that APC/C might be activated. Indeed, rapamycin also induced degradation of another APC/C substrate Clb5 (cyclin B5) in nocodazole-arrested cells (Figure 2A). First, we assessed a possibility that rapamycin causes SAC deactivation and thereby APC/C-Cdc20 activation. However, the SAC proteins Bub1 and Mad2 were still localized on kinetochores after rapamycin treatment (Figures 2B–2D), indicating that the SAC is still active after rapamycin treatment.

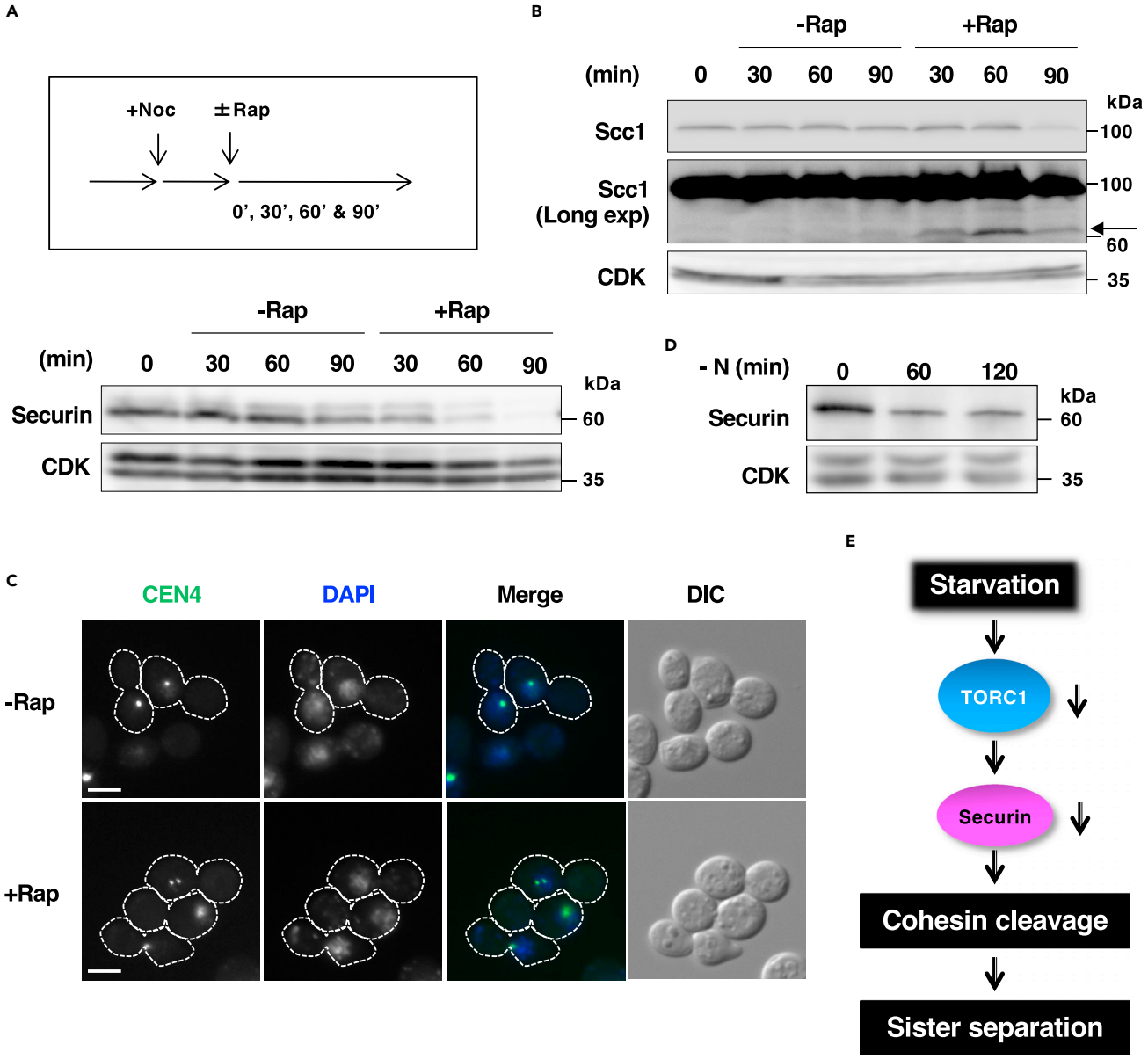

Figure 1. TORC1 inactivation overrides SAC-mediated metaphase arrest

(A) Exponentially growing cells of strain SCU2755 (PDS1-3HA) were arrested in metaphase by nocodazole treatment for 3 h at 30°C. Thereafter, cells were treated with or without rapamycin for the indicated times. 3HA-tagged securin/Pds1 was detected by western blotting analysis using an anti-HA antibody. CDK was detected as a loading control.

(B) Cells of strain SCU1964 (SCC1-TAP) were treated as described in (A). Cleaved products of Scc1 (shown by an arrow) were detected in a long-exposure image using an anti-TAP antibody (PAP).

(C) Cells of strain SCU69 (CEN4-GFP), of which the vicinity of the centromere of chromosome IV was labeled with GFP, were arrested in metaphase as described in (A) and then incubated with or without rapamycin for 1 h. Images of cells, GFP and DAPI were captured using a microscope. Scale bar, 2.5 μm. Separated sister centromeres were counted and are expressed as percentages in Figure 2G, WT.

(D) Cells of strain SCU2755 (PDS1-3HA) were arrested in metaphase and transferred to nitrogen-free media containing nocodazole.

(E) Model of TORC inactivation-induced anaphase onset. Nutrient starvation sequentially causes the inactivation of TORC1, securin degradation, cohesin cleavage, and sister separation.

Rapamycin-induced anaphase onset occurred slowly compared with nocodazole removal-induced anaphase onset: most securin molecules were degraded by 30 min after nocodazole removal (thereafter securin again increased in the next cell cycle after 60 min), whereas some securin molecules remained 30 min after rapamycin treatment (Figure 2E, WT). Important, securin degradation after nocodazole

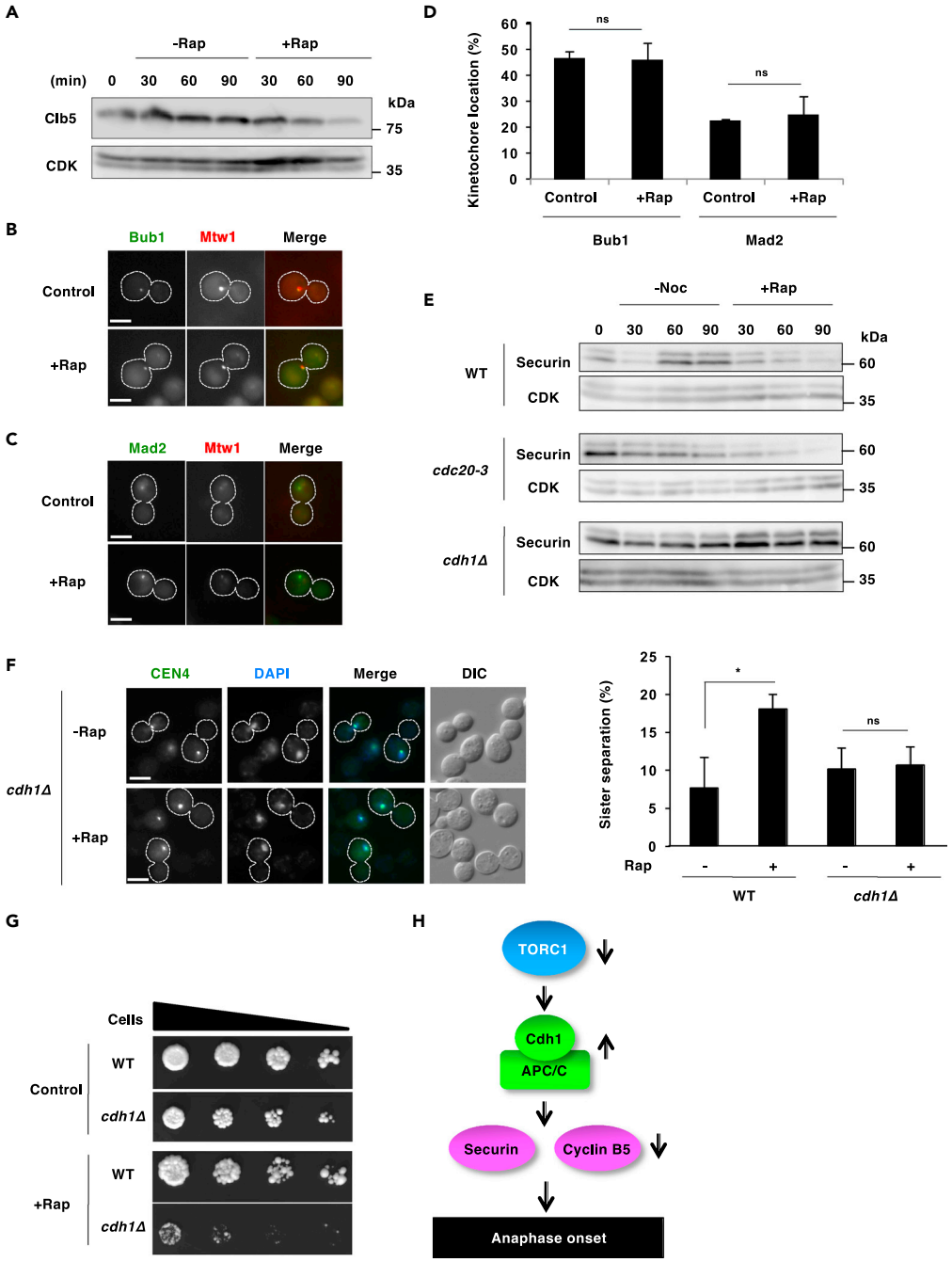

Figure 2. APC/C-Cdh1 mediates TORC1 inactivation-induced anaphase onset

(A) Cells of strain SCU1712 (CLB5-TAP) were treated as described in Figure 1A. TAP-tagged cyclin B5 (Clb5) was detected by western blotting analysis using the anti-TAP antibody (PAP).

(B–D) Cells of strains SCU1485 (BUB1-GFP) and SCU1337 (MAD2-GFP) harboring plasmid pSCU1701 (pMTW1-RFP) were treated as described in Figure 1C. Bub1-GFP and Mad2-GFP signals were captured with Mtw1-RFP (a kinetochore marker) signals. Scale bar, 2.5 μm. Percentages of cells with Bub1-GFP or Mad2-GFP on the kinetochore were determined, and averages and error bars from two independent experiments are shown. Statistical analyses were carried out using the two-tailed Fisher's exact test. ns, not statistically significant.

(E) Cells of strains SCU2755 (PDS1-3HA) and SCU2693 (PDS1-3HA cdc20-3) precultured at 25°C were arrested in metaphase by nocodazole treatment for 3 h and transferred to 37°C for 30 min. Thereafter, cells were treated with rapamycin (+Rap) or released into nocodazole-free media (-Noc) (Time 0). Cells of strain SCU2282 (PDS1-3HA cdh1Δ)

Figure 2. *Continued*

were treated as described in Figure 1A. For comparison, see Figure 1A, WT. 3HA-tagged securin Pds1 was detected by western blotting analysis using the anti-HA antibody.

(F) Cells of strains SCU69 (CEN4-GFP) and SCU2114 (CEN4-GFP cdh1Δ) were treated as described in Figure 1C. Scale bar, 2.5 μm. Percentages of cells with separated sister chromatids were determined and averages and error bars from two independent experiments are shown. Statistical analyses were carried out using the two-tailed Fisher's exact test. *, $p < 0.05$.

(G) Five-fold serial dilutions of cells were spotted in 1-μL drops onto YPAD plates with or without 5 ng/mL rapamycin. The plates were incubated at 30°C for 1 day for YPAD plates and 2 days for rapamycin-containing YPAD plates. The yeast strains SCU893 (wild type) and SCU1228 (cdh1Δ) were used.

(H) Model of APC/C-Cdh1 mediating TORC1 inactivation-induced anaphase onset. The inactivation of TORC1 sequentially causes APC/C-Cdh1 activation, degradation of securin and cyclin B5, and anaphase onset.

removal (SAC deactivation) was suppressed by a *cdc20-3* mutation, whereas securin degradation after rapamycin addition was not suppressed by this mutation (Figure 2E). This demonstrated that TORC1 inactivation-induced anaphase onset was independent of Cdc20.

Recently, we have found that Cdh1 already has a partial activity in metaphase, and if Cdh1 is further activated in metaphase, APC/C-Cdh1 causes mitotic slippage with the SAC being active (Nagai and Ushimaru, 2014; Toda et al., 2012). We suspected that rapamycin evokes Cdh1-mediated mitotic slippage in metaphase cells arrested by the SAC. This was indeed the case: deletion of *CDH1* completely repressed rapamycin-induced securin degradation and sister chromatid separation (Figures 2E and 2F). These findings demonstrated that TORC1 inactivation caused Cdh1-mediated mitotic slippage. We found that *cdh1Δ* cells were hypersensitive to rapamycin (Figure 2G). This indicated that Cdh1 is essential for cell cycle progression, in which TORC1 activity is repressed, and supported the interconnection between TORC1 and Cdh1. Collectively, TORC1 inactivation provoked aberrant APC/C-Cdh1-dependent anaphase onset (Figure 2H).

As for a normal anaphase-telophase transition, Cdh1 is dephosphorylated and relocated from the cytoplasm to the nucleus (Jaspersen et al., 1999). However, no significant dephosphorylation and relocation of Cdh1 was detectable after rapamycin treatment (data not shown). It was likely that TORC1 inactivation caused a partial, but not full, activation of Cdh1. This was consistent with the observation of the slow progression of metaphase-anaphase transition after rapamycin treatment.

Cdc14 mediates TORC1 inactivation-induced anaphase onset

Cdh1 is dephosphorylated and activated by Cdc14 at telophase onset in a normal cell cycle (Jaspersen et al., 1999; Visintin et al., 1998). We found previously that Cdh1-mediated mitotic slippage in *bub2Δ* cells was dependent on Cdc14 (Toda et al., 2012). We suspected that Cdc14 is also involved in the case of rapamycin-induced anaphase onset. In fact, rapamycin-induced, but not nocodazole removal-induced, securin degradation and sister chromatid separation were repressed in *cdc14-1* mutant cells (Figures 3A–3C). Thus, Cdc14 mediated TORC1 inactivation-induced anaphase onset in SAC-active metaphase cells.

In a normal cell cycle, Cdc14 is released from the nucleolus into the nucleus and activated via the Cdc14 early release (FEAR) pathway in early anaphase, and Cdc14 further diffuses throughout the cells via the MEN pathway at telophase onset, and cytoplasmic Cdc14 effectively dephosphorylates Cdh1 localized in the cytoplasm (Bosl and Li, 2005; D'Amours and Amon, 2004). Rapamycin promoted Cdc14 diffusion from the nucleolus (Figures 3D and 3E). This indicated that Cdc14 is activated by TORC1 inactivation. In the case of nocodazole removal, Cdc14 diffused from the nucleolus throughout the cell, whereas in the case of rapamycin treatment, diffused Cdc14 was resident only in the nucleus (Figure S2A). Nuclear-localized Cdc14 could not efficiently dephosphorylate cytoplasmic Cdh1, consistent with the partial activation of Cdh1 after TORC1 inactivation. Consistently, Cdc14 function was critical for cell proliferation, when TORC1 activity was repressed: *cdc14-1* cells were hypersensitive to rapamycin at permissive temperatures (Figure 3F). Here we used cells lacking autophagy-related Atg1 as a control: *atg1Δ* cells were also hypersensitive to rapamycin (Figure 3F), similar to *atg7Δ* cells (in preparation). Overall, these findings suggested that Cdc14 is activated by TORC1 inactivation, promoting anaphase onset via APC/C-Cdh1-mediated securin degradation (Figure 3G).

TORC1 inactivation evokes Net1 degradation

Cdc14 is sequestered in the nucleolus by the nucleolar protein Net1 until metaphase, but when in early anaphase Net1 is phosphorylated, and Cdc14 is released from Net1 (Azzam et al., 2004; Shou et al.,

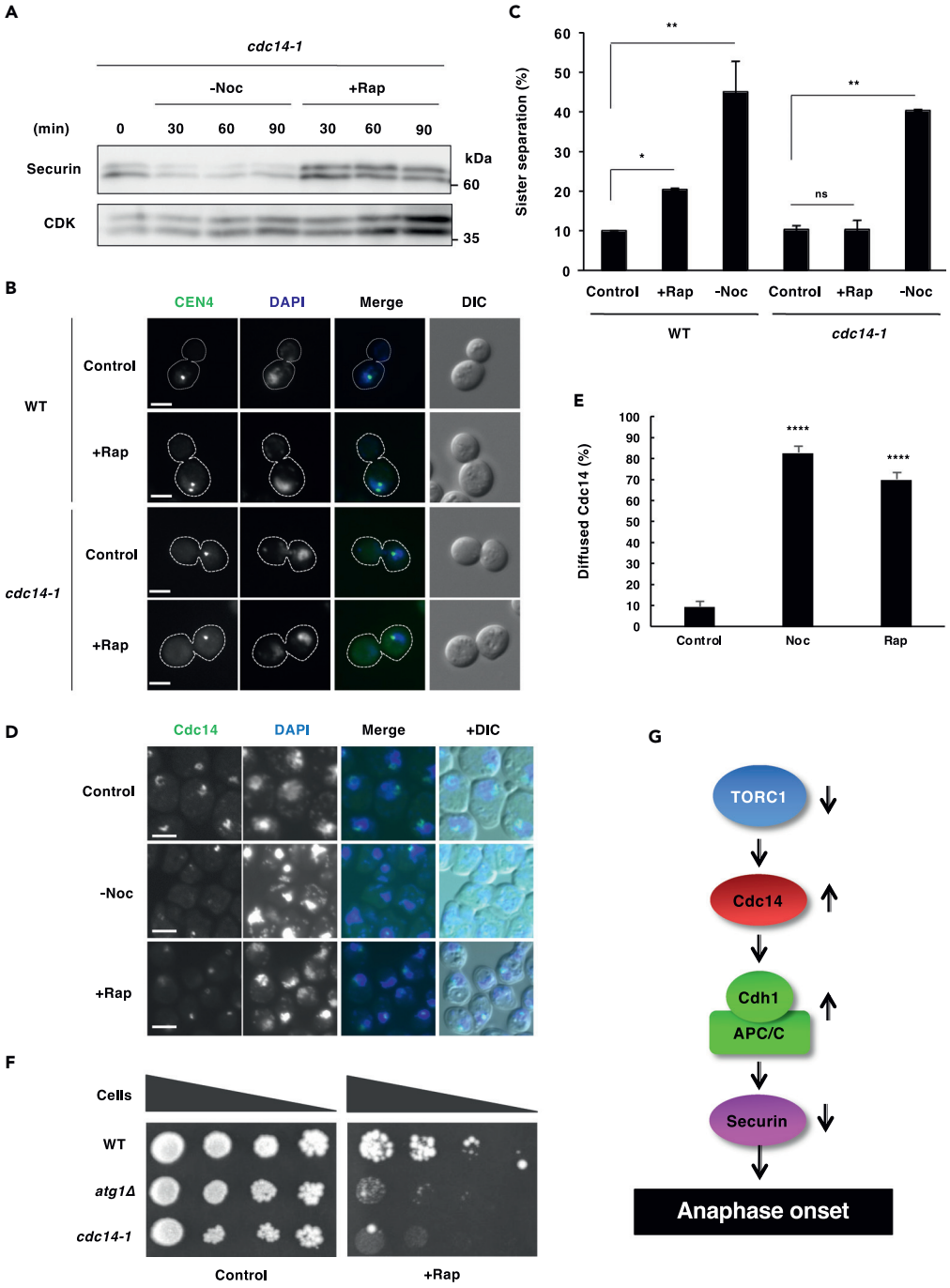

Figure 3. Cdc14 mediates TORC1 inactivation-induced anaphase onset

(A) Cells of strain SCU3250 (PDS1-3HA cdc14-1) were treated as described in Figure 2E. 3HA-tagged securin Pds1 was detected by western blotting analysis using the anti-HA antibody.

(B and C) Cells of strains SCU69 (CEN4-GFP) and SCU3204 (CEN4-GFP cdc14-1) preincubated at 25°C were arrested in metaphase by nocodazole treatment for 3 h and then transferred to 37°C for 30 min. Thereafter, the cells were further incubated with or without rapamycin for 1 h. Scale bar, 2.5 μm. Percentages of cells with separated sister chromatids are shown in (C). For the control, cells were observed 30 min after nocodazole removal. Averages and error bars from two independent experiments are shown. Statistical analyses were carried out using the two-tailed Fisher's exact test. *, $p < 0.05$; **; $p < 0.0001$.

(D and E) Cells of strain SCU1000 (CDC14-5GFP) were treated as described in Figure 1C. Scale bar, 2.5 μm. Percentages of cells with diffused Cdc14 were determined and averages and SD from three independent experiments are shown in (E).

Figure 3. *Continued*
For the control, cells were observed 30 min after nocodazole removal. Statistical analyses were carried out using the two-tailed Fisher's exact test. ****, p <0.000001.
(F) Five-fold serial dilutions of cells of strains SCU893 (wild type) and SCU1001 (cdc14-1) were spotted in 1-μL drops onto YPAD plates with or without 10 ng/mL rapamycin. The plates were incubated at 25°C for 3 days. An unrelated atg1Δ strain (SCU4067) defective in autophagy was used as the control.
(G) Model of Cdc14 mediating TORC1 inactivation-induced anaphase onset. The inactivation of TORC1 sequentially causes Cdc14 activation, APC/C-Cdh1 activation, securin degradation, and anaphase onset.

1999, 2002; Stegmeier et al., 2002; Visintin et al., 1999). Because TORC1 inactivation promotes Cdc14 release from the nucleolus, we suspected that TORC1 inactivation impacted on Net1. Surprisingly, Net1 was lost in nocodazole-treated metaphase cells after rapamycin treatment (Figure 4A). Nitrogen depletion similarly reduced Net1 levels (Figure 4B). We found that Net1 was unstable (Figure 4C). Of note, rapamycin accelerated Net1 degradation in metaphase cells (Figure 4D). These findings showed that TORC1 inactivation promoted Net1 degradation, causing Cdc14 release from Net1, namely, from the nucleolus. Net1 degradation is repressed by treatment with the proteasome inhibitor MG132, but not a deletion of autophagy-related *ATG1* gene (Figures S3A and S3B). This indicated that Net1 is degraded by proteasome but not autophagy.

Because Cdc14 reverses CDK-mediated protein phosphorylation, deregulation of Cdc14 is lethal. In this context, a temperature-sensitive $CDC14^{TAB6\text{-}1}$ mutant defective in the interaction of Cdc14 with Net1 was lethal at restrictive temperatures (Shou and Deshaies, 2002). $CDC14^{TAB6\text{-}1}$ cells were hypersensitive to rapamycin even at permissive temperatures (Figure 4E). This supported the idea that TORC1 inactivation reduced the interaction between Net1 and Cdc14.

Net1 degradation promotes Cdc14 release in SAC-mediated metaphase cells

We wondered if Net1 degradation after rapamycin treatment is sufficient for Cdc14 release. To assess this idea, we determined whether a forced degradation of Net1 also caused Cdc14 release, like rapamycin treatment, using an auxin-induced degron (AID) system (Nishimura et al., 2009). Net1-mediated Cdc14 sequestration is critical for cell proliferation (Shou et al., 1999). Consistently, *net1-aid* cells were sick when Net1 degradation was induced by treatment with 1-naphthaleneacetic acid (NAA) (Figure 5A). After NAA treatment, Net1-aid protein was rapidly lost in asynchronously growing cells and nocodazole-treated metaphase cells (Figures 5B and 5C). This forced degradation of Net1 in metaphase caused Cdc14 diffusion from the nucleolus (Figure 5D). Of importance, Cdc14 diffused to the nucleus but not into the cytoplasm (Figure S2B), as seen with rapamycin treatment, indicating that AID-mediated Net1 degradation in metaphase cells might mimic rapamycin treatment. Furthermore, sister chromatid separation was accelerated under these conditions (Figure 5E), although no remarkable decrease in protein levels of securin was observed (data not shown). Collectively, we concluded that Net1 degradation was sufficient for Cdc14 release and mitotic slippage in SAC-active metaphase cells.

TORC1 inactivation elicits mitotic exit

TORC1 inactivation partially stimulated APC/C-Cdh1 activity. As for a normal mitotic exit, APC/C-Cdh1 mediates cyclin B2 (Clb2) degradation, which triggers mitotic exit. When rapamycin was added to nocodazole-treated metaphase cells, cyclin B2 was also degraded, similar to securin and cyclin B5 (Figure 6A). Consistently, the appearance of G1 cells was significantly increased after rapamycin treatment (Figures 6B–6D). Similarly, nitrogen starvation promoted mitotic exit of nocodazole-treated cells (Figures 6B–6D). Thus, nutrient starvation and TORC1 inactivation promoted not only anaphase onset but also mitotic exit in SAC-active metaphase cells. Collectively, we propose a model for the molecular mechanisms of TORC1 inactivation-induced anaphase onset and mitotic exit: nutrient starvation → TORC1 inactivation → Net1 degradation → Cdc14 release → APC/C-Cdh1 activation → securin and cyclin B2 degradation → anaphase onset and mitotic exit (Figure 6E). Thus, when cells suffer from nutrient starvation, they undergo mitotic slippage to enter into G1 via this aberrant route.

It could be suspected that TORC1 inactivation-induced mitotic slippage might cause chromosome missegregation and reduction in cell viability, because TORC1 inactivation may forcedly promote sister separation despite the presence of insufficient microtubule-kinetochore connections. It was reported that longer-term treatments of rapamycin increased chromosome missegregation (Bonatti et al., 1998; Choi et al., 2000), whereas short-term treatment (1 h) of rapamycin did not significantly induce chromosome

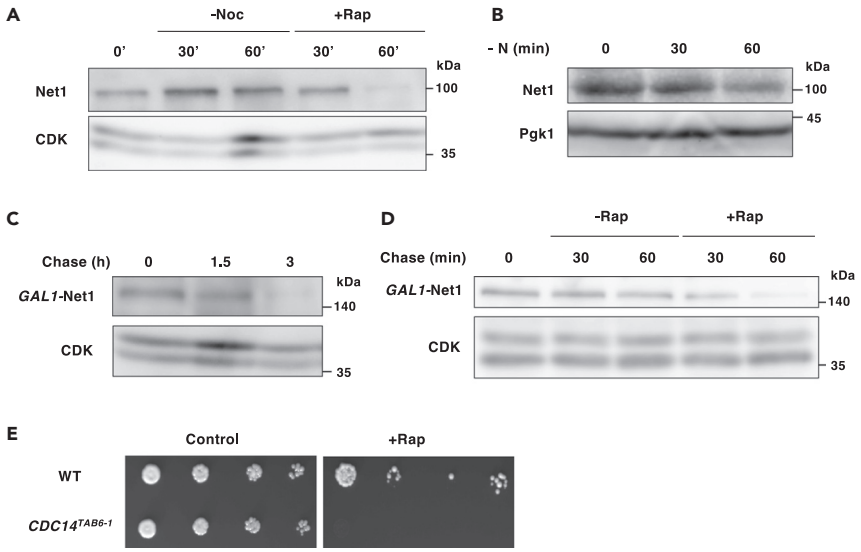

Figure 4. TORC1 inactivation evokes Net1 degradation

(A) Nocodazole-treated metaphase cells of strain SCU3260 (NET1-3HA) were treated with rapamycin or released into nocodazole-free media. 3HA-tagged Net1 was detected using the anti-HA antibody.

(B) Cells of strain SCU7048 (NET1-3HA) arrested in metaphase by nocodazole treatment were transferred to nitrogen-free media containing nocodazole. Pgk1 was detected as a loading control.

(C) Cells of the wild-type strain SCU893 harboring plasmid pSCU1819 (pGAL1-NET1-H6HAZZ) preincubated in a raffinose-based medium were supplemented with 0.01% galactose for 1 h for induction of NET1-H6HAZZ. Protein stabilization of Net1 was assessed after shutoff of NET1-H6HAZZ expression by glucose (2%) addition (time 0). Net1 levels were detected using the anti-ZZ antibody (PAP).

(D) Cells of the wild-type strain SCU893 harboring pSCU1819 (pGAL1-NET1-H6HAZZ) preincubated in raffinose-based medium were arrested in metaphase by nocodazole treatment for 3 h. Thereafter, cells were supplemented with 0.01% galactose for 1 h for induction of NET1-H6HAZZ. Protein stabilization of Net1 was assessed in the presence or absence of rapamycin after shutoff of NET1-H6HAZZ expression by glucose addition (time 0).

(E) Five-fold serial dilutions of cells were spotted in 1-μL drops onto YPAD plates with or without 5 ng/mL rapamycin. The plates were incubated at 30°C for 1 day for YPAD plates and 2 days for rapamycin-containing YPAD plates. The yeast strains SCU893 (wild type) and SCU1199 (CDC14TAB6-1) were used.

missegregation (Figure 6F). However, rapamycin treatment exacerbated chromosome instability in the presence of nocodazole (Figure 6F), and rapamycin remarkably reduced cell viability only in the co-presence of nocodazole (Figure 6G). Thus, TORC1 inactivation exaggerated chromosome instability in conditions in which microtubule-kinetochore attachment was impaired.

mTORC1 inactivation elicits mitotic exit in human cells, which is not dependent on APC/C-Cdh1

We suspected that TORC1 inactivation-invoked mitotic slippage is conserved among eukaryotic cells. To address this question, we examined whether mammalian TORC1 (mTORC1) inactivation overrides SAC-mediated mitotic arrest in human cells. In human cells, it was reported that mitotic slippage occurs as a result of a decreased level of cyclin B below the threshold required to keep cells in mitosis, due to incomplete penetrance of the SAC (Brito and Rieder, 2006). We treated lung cancer-derived A549 cells with rapamycin, following nocodazole treatment (Figure 7A). After prolonged mitotic arrest, cells either die (mitotic cell death) or enter into the next cell cycle (mitotic slippage), which varies not only between different cell lines but also between cells among the same cell line (Gascoigne and Taylor, 2008). Whether cells undergo mitotic cell death or mitotic slippage is explained by the competing networks model, in which cell fate is determined by the competition between cyclin B degradation and pro-apoptotic signal accumulation (Huang et al., 2010; Topham and Taylor, 2013). We observed cells that were in interphase at the beginning of imaging and tracked them for 60 h in live cell imaging. Fates of these cells were judged by their morphology, which were classified into five categories: (1) stayed in interphase throughout the time course, (2) died in interphase, (3) mitotic cell death, (4) mitotic slippage, and (5) stayed in mitosis at the end of imaging (Figures 7B and 7C, Figure S4A). We validated mTORC1 inhibition by the suppression of p70S6K

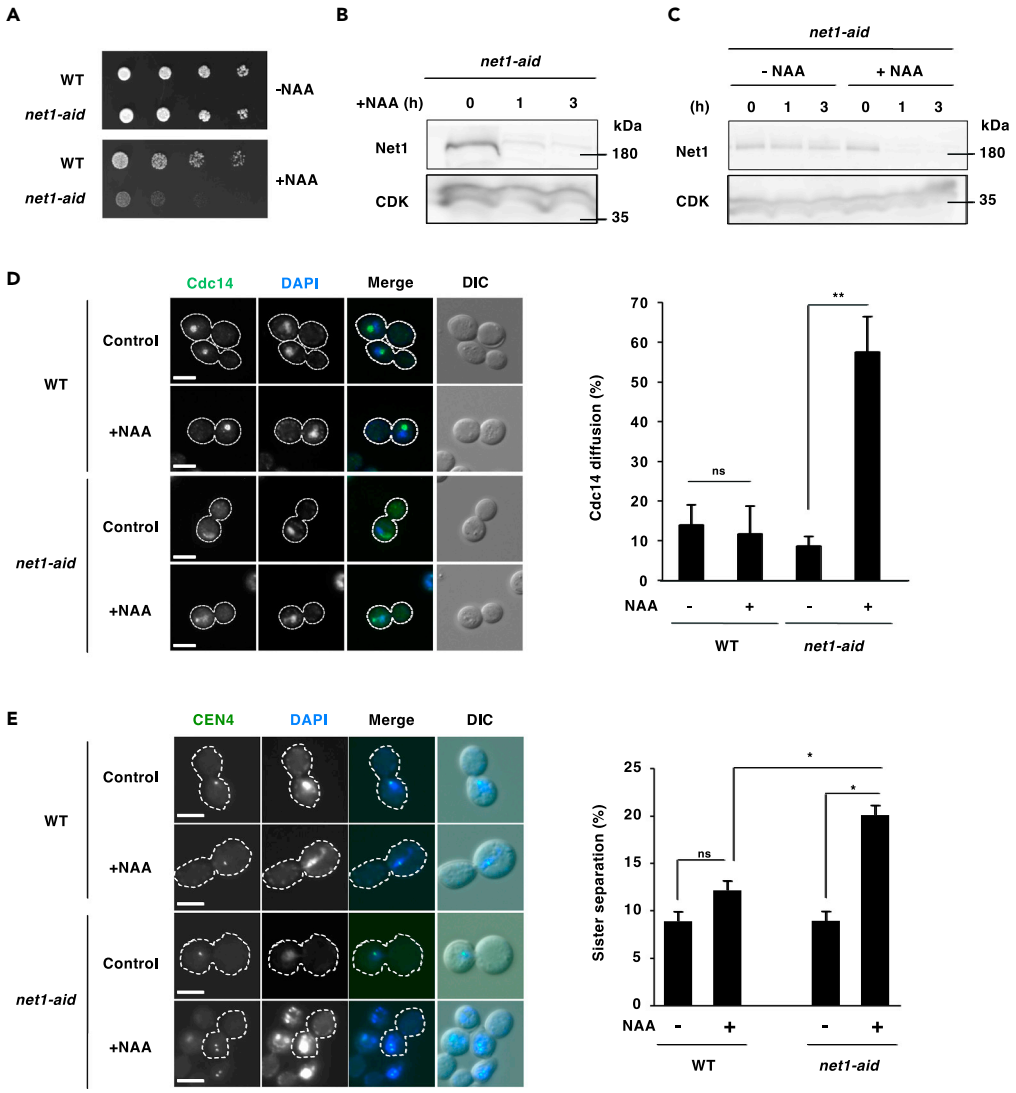

Figure 5. Net1 degradation elicits Cdc14 release in SAC-mediated metaphase cells

(A) Five-fold serial dilutions of cells of strains SCU893 (NET1) and SCU3331 (net1-aid) were spotted in 1-μL drops onto YPAD plates with or without 1 mM 1-naphthaleneacetic acid (NAA). The plates were incubated at 30°C for 1 day.

(B) Cells of strain SCU3331 (net1-aid) were treated with 1 mM NAA. Net1 levels were followed by western blotting analysis using an anti-IAA17 antibody.

(C) Cells of strain SCU3331 (net1-aid) were arrested in metaphase by nocodazole treatment for 3 h and then Net1 degradation was induced by 1 mM NAA treatment (time 0).

(D) Cells of strain SCU3409 (CDC14-5GFP net1-aid) were arrested in metaphase by nocodazole treatment for 3 h and then Net1 degradation was induced by 1 mM NAA treatment (time 0). Scale bar, 2.5 μm. Percentages of cells with diffused Cdc14 were determined and averages and error bars from two independent experiments are shown. Statistical analyses were carried out using the two-tailed Fisher's exact test. **, $p < 0.0001$.

(E) Cells of strains SCU69 (CEN4-GFP) and SCU6232 (net1-aid CEN4-GFP) were arrested in metaphase by nocodazole treatment for 3 h at 30°C and then incubated with or without NAA for 1 h. Scale bar, 2.5 μm. Separated sister centromeres were counted and are expressed as percentages. Averages and SDs from three independent experiments are shown. Statistical analyses were carried out using the two-way ANOVA with Bonferroni correction. *, $p < 0.01$.

phosphorylation (Figure S4B). In mock-treated cells, 33.16 ± 1.33% (SE, n = 4) of cells exhibited mitotic slippage among cells that underwent mitotic cell death or mitotic slippage (Figures 7C and 7D, Mock -Rap). The duration of mitosis was comparable between cells that underwent mitotic cell death and mitotic slippage (Figure 7E, Mock -Rap). The majority of the cells that underwent mitotic slippage died or stayed in interphase after slippage, and only one cell entered mitosis again (Figure S4A, Mock -Rap). In the presence

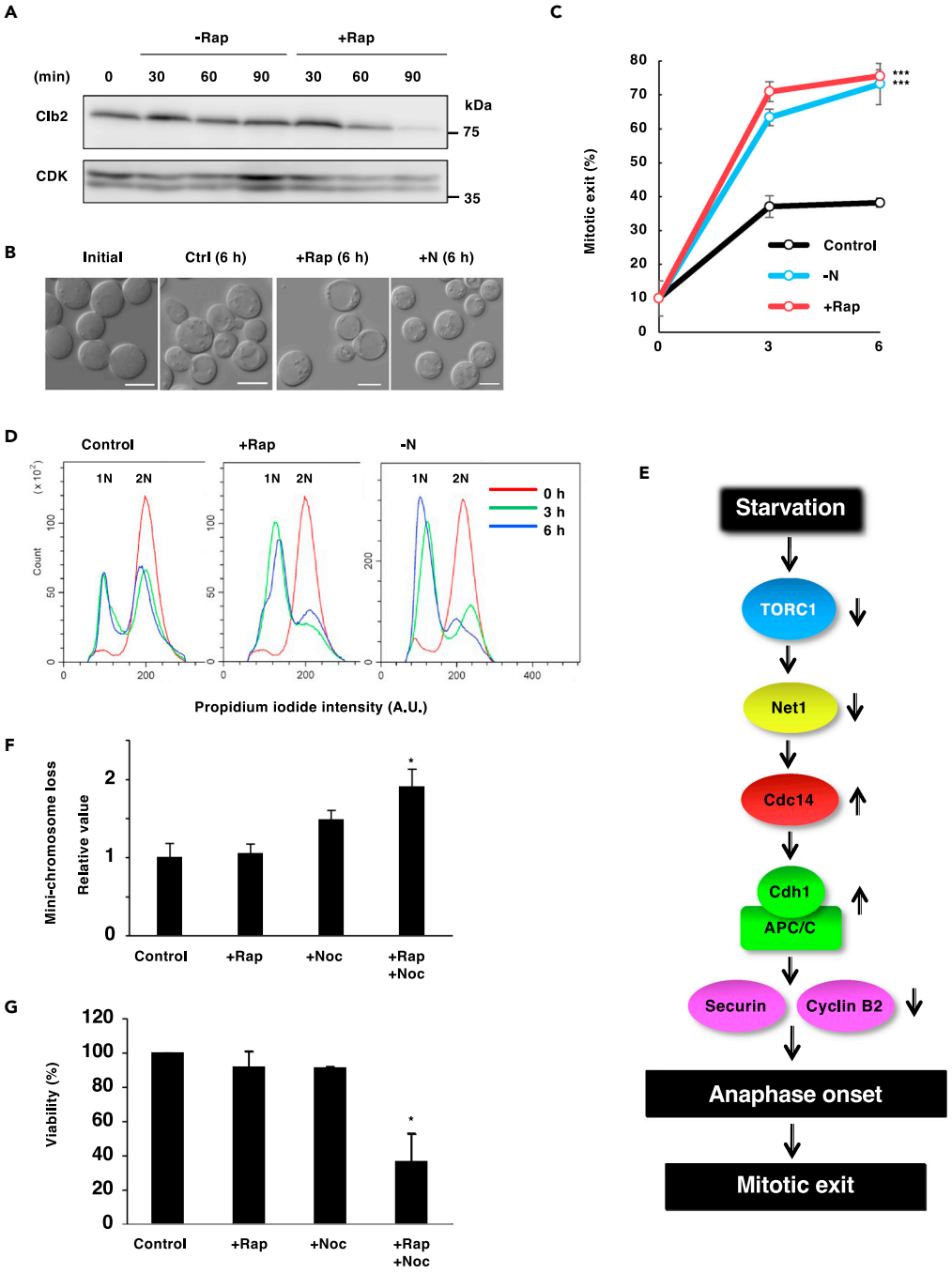

Figure 6. TORC1 inactivation elicits mitotic slippage

(A) Cells of strain SCU1709 (CLB2-TAP) were treated as described in Figure 1A. TAP-tagged cyclin B2 (Clb2) was detected by western blotting analysis using the anti-TAP antibody.

(B and C) Cells of the wild-type strain SCU893 were arrested in metaphase by nocodazole treatment for 3 h and then further cultured with or without (control) rapamycin, or in nitrogen-depleted media (SD-N) (time 0) for the indicated times. Scale bar, 2.5 μm. Percentages of G1 cells without buds were determined and averages and SDs from three independent experiments are shown in (C). p Values were calculated using the two-way ANOVA with Bonferroni correction. ***, $p < 0.0005$.

(D) Cells of wild-type strain SCU893 were cultured as described in (B) and subjected to flow cytometric analysis. Accumulation of G1 cells after rapamycin treatment or nitrogen starvation was assessed.

(E) Model in which the inactivation of TORC1 elicits mitotic slippage.

Figure 6. *Continued*

(F) The chromosome instability (CIN) assay using a tester strain SCU1237 was performed as described in STAR Methods." Percentages of cells that lost their mini-chromosomes were determined, and averages and error bars from two independent experiments are shown. Statistical analyses were carried out using the two-tailed Fisher's exact test. *, $p < 0.05$.

(G) Cells of strain SCU893 (wild type) were treated with rapamycin (200 ng/mL) and/or nocodazole (10 μg/mL) for 1 h. Thereafter, for detection of cell viability, cells were spread on the YPAD plate and incubated for 3 d at 30°C. The number of colonies formed from surviving cells was counted, and averages and error bars from two independent experiments are shown. Statistical analyses were carried out using the two-tailed Fisher's exact test. *, $p < 0.01$.

of rapamycin, there was a slight increase in the proportion of cells that stayed in interphase, which may be due to the inhibition of G1 phase progression by mTORC1 pathway (Fingar et al., 2004) (Figure 7C, Mock + Rap). Intriguingly, the rate of mitotic slippage increased to 46.41 ± 1.87% (S.E., n = 4) by rapamycin treatment (Figures 7C and 7D, Mock + Rap). This suggested that mTORC1 inhibition elicits mitotic exit in human cells, as in yeast cells. The level of Mad1, a SAC protein, on kinetochores did not decrease after rapamycin treatment (Figures S5A–S5C), excluding the possibility that rapamycin directly affects the SAC. The duration of mitosis before mitotic slippage in rapamycin-treated cells was comparable with that in mock-treated cells (Figure 7E, Mock + Rap), suggesting that the increase in the rate of mitotic slippage is not due to accelerated cyclin B degradation. Consistent with the possibility, the level of cyclin B in rapamycin-treated cells was comparable with that in mock-treated cells (Figures S5D and S5E). These data suggested that increased mitotic slippage by rapamycin treatment is probably through the alteration in the balance between mitotic slippage and mitotic cell death.

To address the relationship between mTORC1 and APC/C-Cdh1 in human cells, we also observed Cdh1-depleted cells (Figures 7B and 7C, Figures S4A and S4B, siCdh1 -Rap). Cells that died in interphase increased significantly, which might be related to the role of APC/C-Cdh1 in the maintenance of G1 phase (Qiao et al., 2010). In contrast to the results in yeast, Cdh1 depletion rather increased mitotic slippage to 46.36 ± 2.79% (SE, n = 4), comparable with that in rapamycin-treated cells (Figures 7C and 7D siCdh1 -Rap). The duration of mitosis before mitotic slippage did not significantly shorten (Figure 7E, siCdh1 -Rap), suggesting that cyclin B degradation was not accelerated, similarly to rapamycin treatment. In contrast, the duration of mitotic arrest before cell death was markedly reduced in Cdh1-depleted cells (Figure 7E, siCdh1 -Rap). Furthermore, cells that underwent mitotic slippage died earlier in interphase after mitotic slippage compared with mock-treated cells (Figure 7F, siCdh1 -Rap). Therefore, the increase in the rate of mitotic slippage did not contribute to overall cell survival. Rapamycin treatment in Cdh1-depleted cells further reduced the fraction of cells that entered mitosis because of the increase in cells that stayed in interphase and did not result in further increase in the rate of mitotic slippage (52.77 ± 2.31% [SE, n = 4], Figures 7C and 7D, siCdh1 +Rap). The duration of mitotic arrest before mitotic cell death and duration of interphase after mitotic slippage were similarly reduced in Cdh1-depleted cells with or without rapamycin treatment (Figures 7E and 7F, siCdh1 -Rap vs siCdh1 +Rap). These data suggested that both mTORC1 inhibition and APC/C-Cdh1 depletion facilitate mitotic slippage, which is supposedly due to changes in the balance between mitotic slippage and cell death. However, Cdh1 depletion showed additional effects on the overall cell survival after mitotic arrest.

We also observed cells depleted of Cdc20, which is crucial for mitotic exit. Consistent with the previous report (Huang et al., 2009), nearly all cells that entered mitosis died, and mitotic slippage was rarely seen (Figure 7C, siCdc20 -Rap). The situation was the same in the presence of rapamycin (Figure 7C, siCdc20 Rap), or when Cdh1 was simultaneously depleted (Figure 7C, siCdh1+siCdc20 -Rap and siCdh1+ siCdc20 + Rap). These data confirmed that Cdc20 depletion eliminates mitotic slippage altogether, regardless of the underlying causes. To verify that this is due to inhibition of cyclin B degradation, we observed nocodazole-treated cells in the presence of MG132, a proteasome inhibitor (Figure S5A). We confirmed that cyclin B level was increased upon MG132 treatment (Figures S5D and S5E). Kinetochore localization of Mad1 was also increased, in line with a recent finding that cyclin B1 scaffolds Mad1 at the kinetochore (Figures S5B and S5C) (Allan et al., 2020). Live cell imaging revealed that no cells underwent mitotic slippage in the presence of MG132 (Figure S5F), corroborating that cyclin B degradation, which is induced by APC/C-Cdc20 in physiological conditions, is required for mitotic slippage. Collectively, our data suggested that mTORC1 inactivation invoked mitotic slippage both in yeast and human cells, although it is mediated by APC/C-Cdh1 in yeast cells but not in human cells.

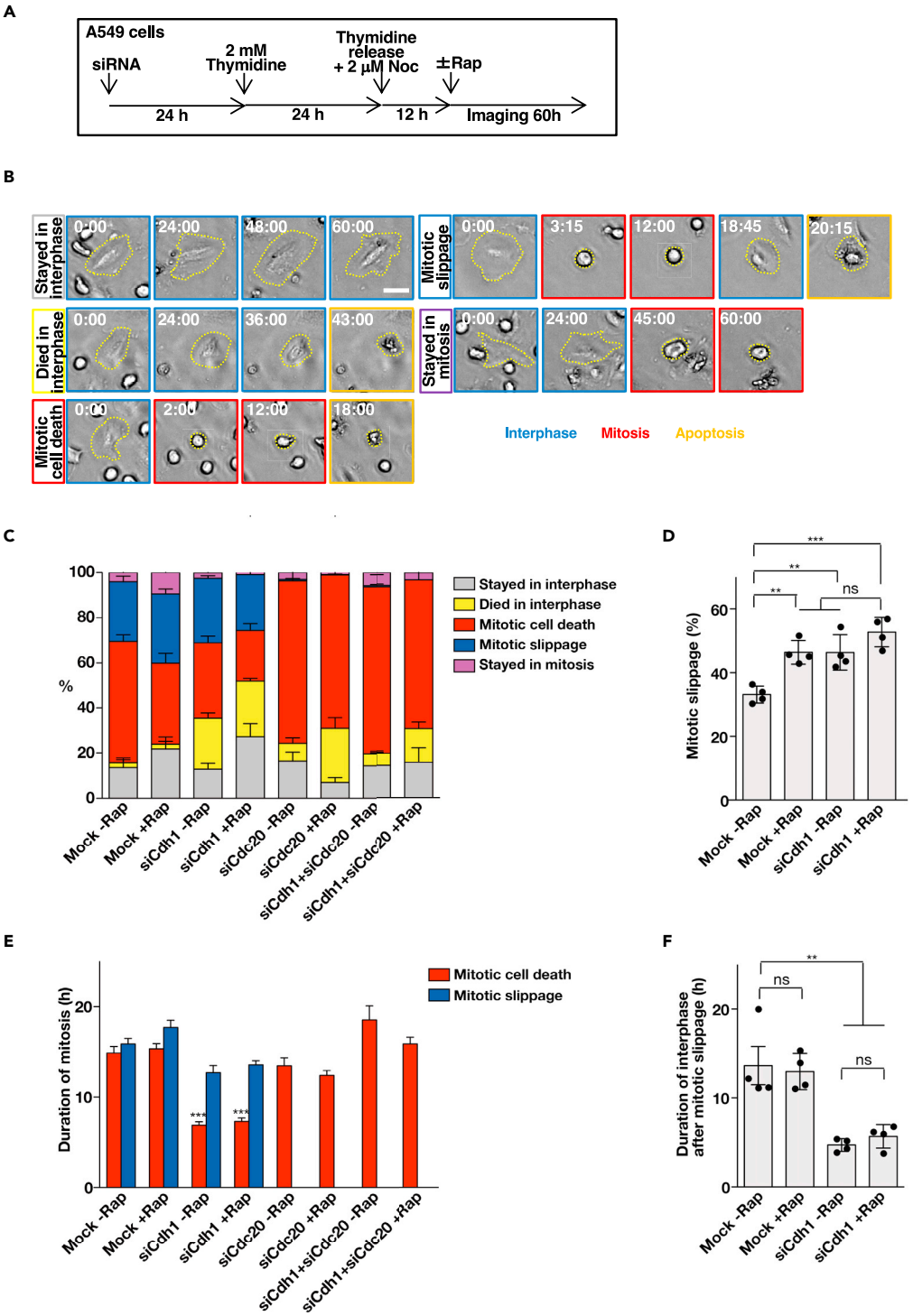

Figure 7. mTORC1 inactivation elicits mitotic slippage

(A) A schematic of the experimental procedure.

(B) Phase-contrast time-lapse imaging of nocodazole-treated A549 cells. An example representing each category of cell fate to classify cells in Figure S4A is shown. Numbers show elapsed time (hour:minute) relative to the start of imaging. Scale bar, 50 μm.

(C) Fate of nocodazole-treated A549 cells with or without rapamycin treatment after 60-h imaging. Proportion of cells classified into each category, obtained by averaging the results of four independent experiments shown in Figure S4A, is presented. Error bars represent standard errors.

Figure 7. *Continued*

(D) Rate of mitotic slippage in nocodazole-treated A549 cells with or without rapamycin treatment and/or Cdh1 depletion. Percentage of cells that underwent mitotic slippage among the cells that underwent mitotic cell death or mitotic slippage, obtained by averaging the results of four independent experiments that are shown as dots, is presented. Error bars represent standard errors. **, p <0.01; ***, p <0.001 (Tukey's multiple comparison test). ns, not statistically significant.

(E) Duration of mitosis in nocodazole-treated A549 cells that underwent mitotic cell death or mitotic slippage. The results are average of four independent experiments. The results of rare mitotic slippage events in cells depleted of Cdc20 with or without Cdh1 were not shown. Error bars represent standard errors. ***, p <0.001 (Tukey's multiple comparison test, comparison with Mock -Rap, mitotic cell death).

(F) Duration of interphase after mitotic slippage in nocodazole-treated A549 cells with or without rapamycin treatment and/or Cdh1 depletion. The results are average of four independent experiments, which are shown as dots. Error bars represent standard errors. **, p <0.01 (Tukey's multiple comparison test). ns, not statistically significant.

DISCUSSION

Unconventional aspects of TORC1 inactivation-elicited mitotic slippage in yeast

Here, we showed that starvation-induced TORC1 inactivation promoted mitotic slippage in yeast cells. We proposed a model for its molecular mechanisms (Figure 6E). It should be noted that this TORC1 inactivation-specific pathway includes numerous unconventional aspects: Net1 degradation in metaphase, Cdc14 release in metaphase, and APC/C-Cdh1-mediated anaphase onset and mitotic exit.

APC/C-Cdc20 mediates anaphase onset in a normal cell cycle progression, whereas APC/C-Cdh1 mediates telophase onset (Schwab et al., 1997; Visintin et al., 1997). However, we recently found that APC/C-Cdh1 was partially active in nocodazole-treated metaphase cells (Nagai and Ushimaru, 2014). Furthermore, APC/C-Cdh1 mediated anaphase onset in Bub2-deficient cells (Toda et al., 2012). Bub2 is an inhibitory protein for the MEN pathway, and loss of Bub2 caused precocious APC/C-Cdh1 activation via Cdc14. TORC1 inactivation- and Bub2 deficiency-induced mitotic slippage have some similarities: (1) commitment of Cdc14, (2) APC/C-Cdh1-dependent securin degradation, and (3) slow metaphase-anaphase transition. Securin is degraded after ubiquitination mediated by APC/C-Cdc20 in anaphase and then APC/C-Cdh1 in telophase in a normal cell cycle progression (Nagai and Ushimaru, 2014; Toda et al., 2012) (Figure S6A). Namely, securin degradation is normally initiated by APC/C-Cdc20 at anaphase onset, but it was aberrantly mediated by APC/C-Cdh1 in specific conditions, including nutrient-starved conditions (Figures S6B and S6C). However, TORC1 inactivation- and Bub2 deficiency-induced mitotic slippage have a dissimilarity; Bub2 deficiency caused Cdc14 activation via the MEN pathway (Toda et al., 2012), whereas TORC1 inactivation caused Cdc14 activation via Net1 degradation (this study). We found that TORC1 inactivation induces proteasome-dependent Net1 degradation. Furthermore, after TORC1 inactivation, repression of protein synthesis by reduction in translation initiation and ribosome biogenesis, in addition to autophagic degradation of ribosomes (Beau et al., 2008; Loewith and Hall, 2011), promotes the reduction in Net1 protein levels.

APC/C-Cdc20 normally promotes anaphase onset, and thereafter APC/C-Cdh1 promotes telophase onset (Schwab et al., 1997; Visintin et al., 1997). This sequential activation of APC/C-Cdc20 and APC/C-Cdh1 is the heart of accurate mitosis (Toda et al., 2012). APC/C-Cdc20 recognizes the D-box of a relatively limited number of targets (the critical targets are securin and Clb5 in budding yeast) (Shirayama et al., 1999), whereas APC/C-Cdh1 recognizes various motifs (e.g., KEN box) on numerous targets, including substrates for APC/C-Cdc20 (for example, securin) (Manchado et al., 2010; Pines, 2006; van Leuken et al., 2008; Wasch et al., 2010) (Figure S6A). Therefore, when APC/C-Cdh1 is aberrantly activated in metaphase, APC/C-Cdh1 simultaneously triggers anaphase and telophase onset (Toda et al., 2012) (Figure S6C). In addition, APC/C-Cdh1-mediated anaphase onset caused chromosome missegregation, because anaphase progression occurred despite the presence of insufficient microtubule-kinetochore attachments (this study) (Toda et al., 2012).

Intercommunication between TORC1 and CDK is ambiguous. This study showed that TORC1 inactivation antagonized CDK through two different ways in yeast cells: APC/C-Cdh1-dependent degradation of Clb proteins (decrease in CDK activity itself) and activation of Cdc14 (increase in activity to reverse CDK/Clb-mediated phosphorylation). In other words, TORC1 guaranteed CDK action by repression of Cdc14 and Cdh1 in normal (nutrient-rich) conditions.

Cdc14 antagonizes the TORC1 signaling and is negatively regulated by TORC1

Protein phosphatase 2A (PP2A; Pph21 and Pph22) and the PP2A-related PP6 (Sit4) phosphatases are activated after TORC1 inactivation in budding yeast (Loewith and Hall, 2011; Zoncu et al., 2011). In nutrient-rich

conditions, TORC1 promotes phosphorylation of Tap42, which is an inhibitor of PP2A and PP6 (Jiang and Broach, 1999). Upon TORC1 inactivation, Tap42 dissociates from PP2A and PP6, activating both phosphatases. Thus, PP2A and Sit4 are activated after the inactivation of TORC1 in a Tap42-dependent manner. A global kinase-phosphatase interaction network has suggested that Cdc14 is an antagonist of the TORC1 signaling (Breitkreutz et al., 2010), although the molecular connection between TORC1 and Cdc14 remained unclear. We showed here that Cdc14 is a TORC1-downstream phosphatase: Cdc14 was activated by TORC1 inactivation in a manner different from that in PP2A and PP6. Of note, Cdc14 dephosphorylates TORC1-mediated phosphorylation of the autophagy-related protein Atg13 after TORC1 inactivation (Yeasmin et al., 2016). Collectively, Cdc14 antagonizes the TORC1 signaling and is negatively regulated by TORC1.

Roles of Cdc14 as a stress-responsive protein phosphatase

Cdc14 phosphatase reverses CDK-Clb (cyclin B)-dependent phosphorylation and is essential for mitotic exit in budding yeast (Queralt and Uhlmann, 2008; Stegmeier and Amon, 2004). We found that Cdc14 mediates TORC1 inactivation-induced mitotic slippage in budding yeast, probably through dephosphorylating Cdh1. The fission yeast homolog Clp1/Flp1 is also involved in mitotic exit/cytokinesis (Clifford et al., 2008; Esteban et al., 2004; Wolfe and Gould, 2004). By contrast, the PP2A and PP1 phosphatases are responsible for mitotic exit in animal cells (Grallert et al., 2015; Mochida et al., 2009; Ohkura et al., 1989; Schmitz et al., 2010; Wu et al., 2009). Whether human homolog Cdc14B (hCdc14B) is involved in mitotic exit/cytokinesis is controversial (Dryden et al., 2003; Mocciaro et al., 2010; Rodier et al., 2008).

Aside from this, the Cdc14 family of phosphatases is also involved in DNA stress responses. Mammalian hCdc14B localizes to the nucleolus and is released from the nucleolus in response to DNA damage and dephosphorylates Cdh1 to regulate the DNA damage response (Bassermann et al., 2008; Kaiser et al., 2002; Mocciaro et al., 2010; Peddibhotla et al., 2011; Sudo et al., 2001). Fission yeast Clp1 is also released from the nucleolus to the nucleus in response to DNA replication stress in S phase and is required for the DNA damage responses (Diaz-Cuervo and Bueno, 2008). In budding yeast, a global PKI network analysis suggested that Cdc14 is involved in the DNA damage response (Breitkreutz et al., 2010). We showed herein that yeast Cdc14 promoted mitosis progression in response to starvation. In addition, Cdc14 is required for induction of autophagy (macroautophagy) and micronucleophagy in budding yeast (Kondo et al., 2018; Mostofa et al., 2021). Thus, Cdc14 is a key factor to respond to nutrient stress in budding yeast. In contrast to yeast, human cells undergo an open mitosis and disassemble both the nucleus and nucleolus in mitosis, and hCdc14B is diffused to the cytoplasm in metaphase. Therefore, even if hCdc14B responds to nutrient starvation in metaphase, its molecular mechanism should be completely different from that in budding yeast. Alternatively, it is likely that human Cdc14 is not involved in mitotic slippage.

TORC1 switches nutrient- and starvation-specific mitotic routes toward G1

TORC1 activity is critical for G1/S progression, and starved cells arrest at G1 phase eventually (Barbet et al., 1996; Zinzalla et al., 2007). However, a mounting body of evidence shows that TORC1 regulates cell cycle progression other than G1 progression: TORC1 activity is required for proper S phase progression (DNA replication) and G2/M transition (Matsui et al., 2013; Nakashima et al., 2008; Tran et al., 2010; Yamamoto et al., 2018). Thus, TORC1 activity is required for various aspects of cell cycle phase progression and transition. However, because starved cells have to reach G1 phase, they should progress toward G1 phase albeit slowly.

If starved cells meet with microtubule problems in mitosis, what do cells do: stop at metaphase or override metaphase arrest? The present study demonstrated that starved yeast cells selected to override the SAC-mediated metaphase arrest to go toward G1 (Figures 6B–6D). Starvation-induced TORC1 inactivation opened the emergency exit toward G1. This might be an adaptive response to starvation, albeit at the cost of chromosome missegregation and death in some cells (Figures 6F and 6G). Because yeast cells in a population are clonal, some surviving cells may properly transmit their genome. Cells appeared to prefer to override the SAC, albeit with a risk, than the death of all clonal cells by eternal metaphase arrest. Many studies have been devoted to the analysis of cell cycle progression in laboratory conditions. However, in natural circumstances, organisms including yeast frequently suffer from nutrient starvation, and cells have to switch nutrient- and starvation-specific mitotic progress pathways in response to nutrient availability. We showed here that there is not just one route to lead to G1. In normal (nutrient-rich) conditions, TORC1 closes off the dangerous, starvation-specific route. Thus, TORC1 switches nutrient- (secure) and starvation-specific (dangerous) mitotic routes toward G1 in response to nutrient availability. This study suggested that a similar TORC1-regulated switching system also appears to be conserved

in mammalian cells, although the biological benefits of the starvation-dependent risky route in multicellular organisms is unclear at present.

mTORC1 and mitotic slippage

We found that mTORC1 inhibition also elicits mitotic slippage in human cells. However, the increased mitotic slippage in human cells was not dependent on Cdh1, in contrast to that in yeast cells. Our data expand the idea that TORC1 plays a critical role in mitotic regulation not only in budding yeast but also in mammalian cells (Bonatti et al., 1998; Choi et al., 2000), although how mTORC1 inactivation promotes mitotic slippage in human cells is currently unclear. It has been revealed that mTORC1 is involved not only in G1 phase progression but also in various mitotic processes including G2/M transition, centrosome duplication, spindle assembly, and cytokinesis (Astrinidis et al., 2006; Platani et al., 2018; Ramírez-Valle et al., 2010). Related to these mitotic functions, a number of proteins related to TORC1 signaling are reported to reside at the mitotic apparatus such as centrosomes, spindle midzone, and midbody (Cuyàs et al., 2014). We observed the effect of rapamycin in A549 cells treated with nocodazole to mimic the conditions of yeast experiments. As spindle and midzone are not formed in the presence of nocodazole, the increased mitotic slippage by rapamycin treatment may not be related to the role of mTORC1 in spindle assembly and cytokinesis. Rapamycin treatment elicits premature anaphase onset in yeast cells by overriding active SAC signaling, whereas it facilitates mitotic slippage in human cells at similar timing with mitotic cell death after prolonged mitotic arrest, suggesting that mTORC1 plays a role in the balance between mitotic cell death and mitotic slippage, but not in the timing of anaphase onset.

Cdh1 targets securin in a manner dependent on D/KEN boxes, and our data in yeast cells are consistent with the previous reports that deregulation of Cdh1 in pre-anaphase results in premature securin degradation and sister-chromatid separation (Hagting et al., 2002; Jeganathan et al., 2005; Zur and Brandeis, 2001) (Figure S6C). On the other hand, we found that Cdh1 depletion rather increased the rate of mitotic slippage in human cells. It is plausible that mitotic slippage in human cells is mainly driven by APC/C-Cdc20 (Brito and Rieder, 2006; Huang et al., 2009), and one possibility is that Cdh1 competes with Cdc20 for the activation of APC/C, which may cause increased mitotic slippage upon Cdh1 depletion. Indeed, we found the competition between Cdh1 and Cdc20 in nocodazole-treated metaphase cells in yeast (Nagai and Ushimaru, 2014; Toda et al., 2012). Although both rapamycin treatment and Cdh1 depletion elicited mitotic slippage in human cells, durations of mitotic arrest before cell death and survival time after mitotic slippage were shorter in Cdh1-depleted cells compared with rapamycin-treated cells. They might be due to the link between Cdh1 and apoptosis, because it was reported that Cdh1 depletion enhances susceptibility to apoptosis in several occasions (Eguren et al., 2013; Liu et al., 2008). The increase in the rate of cells that died in interphase upon Cdh1 depletion may also be caused by the enhanced susceptibility to apoptosis. Overall, although Cdh1 depletion increased the rate of mitotic slippage in human cells, it did not contribute to enhanced cell survival.

Concluding remarks

Rapamycin treatment promotes chromosome instability in yeast and mammalian cells (Bonatti et al., 1998; Choi et al., 2000). This study dissected the molecular mechanism of TORC1 inactivation-induced chromosome instability. Rapamycin and other TORC1 inhibitors are used as anti-cancer drugs, in addition to being immunosuppressants (Benjamin et al., 2011; Vignot et al., 2005). However, these drugs might rather increase genome instability in healthy cells, causing tumor progression. We believe that the present results are useful for the anticipation of undesirable side effects of the use of TORC1 inhibitors. In addition, this study demonstrated that the TORC1-APC/C axis is a potent therapeutic target to prevent mitotic slippage in cancer cells in the presence of anti-tumor microtubule poisons.

Limitations of the study

This study demonstrated that the lack of Cdh1 repressed mitotic slippage after TORC1 inactivation in yeast cells, indicating that Cdh1 is required for mitotic slippage. However, we observed no detectable Cdh1 activation (dephosphorylation and relocation to the nucleus) after rapamycin treatment. Changes in Cdh1 features after rapamycin treatment remains to be investigated in the future.

STAR★METHODS

Detailed methods are provided in the online version of this paper and include the following:

SUPPLEMENTAL INFORMATION

Supplemental information can be found online at https://doi.org/10.1016/j.isci.2021.103675.

ACKNOWLEDGMENTS

We thank Angelika Amon, Orna Cohen-Fix, Raymond Deshaies, Kevin Hardwick, Johannes Hegemann, Masato Kanemaki, John McCusker, Danesh Moazed, Andrew Murray, Kim Nasmyth, Booth Quimby, Akio Toh-e, and Mark Winey for generous gifts of materials. We give special thanks to Ayumu Yamamoto, Masahiro Uritani, and laboratory members of T.U. for helpful discussions. This research was partially carried out using instruments at the Institute for Genetic Research and Biotechnology of Shizuoka University. This work was supported in part by the Japan Society for the Promotion of Science (JSPS) (grant No. 19370082, 23570225, 18K06212, 20H05317, and 21H02475 to T.U. and No. 15H04368 to K.T.), MEXT (grant No. 16H01296 to K.T.), the Institute for Fermentation, Osaka (grant No. G-2020-2-055 to T.U.), Takeda Science Foundation Grant (to K.T.), and Tohoku University (the Cooperative Research Project Program of Joint Usage/Research Center at the Institute of Development, Aging and Cancer; grant No. H28-6, H29-26, H30-1, R1-6, R2-95, and R3-1 to T.U.).

AUTHOR CONTRIBUTIONS

T.U. conceived the project and designed the experiments. K.T. designed the experiments using human cells. C.Y., A.M., S. Miyazaki, M.N., S. Mase, K.I., M.N.T., T.T., S.N., S. Morshed, N.K., M.G.M., T.S., H.K., and K.O. performed the experiments and acquired, analyzed, and interpreted the data. M.A.R. provided technical support. T.U. drafted and revised the manuscript. K.T. drafted and revised parts as to experiments using human cells. M.N.T. and T.T. helped to write the revised manuscript. T.U. and K.T. are the guarantors of this work.

DECLARATION OF INTERESTS

The authors declare no competing interests.

Received: December 28, 2020
Revised: October 20, 2021
Accepted: December 20, 2021
Published: February 18, 2022

REFERENCES

Allan, L.A., Camacho Reis, M., Ciossani, G., Huis In 't Veld, P.J., Wohlgemuth, S., Kops, G.J., Musacchio, A., and Saurin, A.T. (2020). Cyclin B1 scaffolds MAD1 at the kinetochore corona to activate the mitotic checkpoint. EMBO J *39*, e103180.

Astrinidis, A., Senapedis, W., and Henske, E.P. (2006). Hamartin, the tuberous sclerosis complex 1 gene product, interacts with polo-like kinase 1 in a phosphorylation-dependent manner. Hum. Mol. Genet. *15*, 287–297.

Azzam, R., Chen, S.L., Shou, W., Mah, A.S., Alexandru, G., Nasmyth, K., Annan, R.S., Carr, S.A., and Deshaies, R.J. (2004). Phosphorylation by cyclin B-Cdk underlies release of mitotic exit activator Cdc14 from the nucleolus. Science *305*, 516–519.

Barbet, N.C., Schneider, U., Helliwell, S.B., Stansfield, I., Tuite, M.F., and Hall, M.N. (1996). TOR controls translation initiation and early G1 progression in yeast. Mol. Biol. Cell *7*, 25–42.

Bassermann, F., Frescas, D., Guardavaccaro, D., Busino, L., Peschiaroli, A., and Pagano, M. (2008). The Cdc14B-Cdh1-Plk1 axis controls the G2 DNA-damage-response checkpoint. Cell *134*, 256–267.

Beau, I., Esclatine, A., and Codogno, P. (2008). Lost to translation: when autophagy targets mature ribosomes. Trends Cell Biol. *18*, 311–314.

Benjamin, D., Colombi, M., Moroni, C., and Hall, M.N. (2011). Rapamycin passes the torch: a new generation of mTOR inhibitors. Nat. Rev. Drug Discov. *10*, 868–880.

Bharadwaj, R., and Yu, H. (2004). The spindle checkpoint, aneuploidy, and cancer. Oncogene *23*, 2016–2027.

Bonatti, S., Simili, M., Galli, A., Bagnato, P., Pigullo, S., Schiestl, R.H., and Abbondandolo, A. (1998). Inhibition of the Mr 70,000 S6 kinase pathway by rapamycin results in chromosome malsegregation in yeast and mammalian cells. Chromosoma *107*, 498–506.

Bosl, W.J., and Li, R. (2005). Mitotic-exit control as an evolved complex system. Cell *121*, 325–333.

Breitkreutz, A., Choi, H., Sharom, J.R., Boucher, L., Neduva, V., Larsen, B., Lin, Z.Y., Breitkreutz, B.J., Stark, C., Liu, G., et al. (2010). A global protein kinase and phosphatase interaction network in yeast. Science *328*, 1043–1046.

Brito, D.A., and Rieder, C.L. (2006). Mitotic checkpoint slippage in humans occurs via cyclin B destruction in the presence of an active checkpoint. Curr. Biol. *16*, 1194–1200.

Brummelkamp, T.R., Bernards, R., and Agami, R. (2002). A system for stable expression of short interfering RNAs in mammalian cells. Science *296*, 550–553.

Choi, J.H., Adames, N.R., Chan, T.F., Zeng, C., Cooper, J.A., and Zheng, X.F. (2000). TOR signaling regulates microtubule structure and function. Curr. Biol. *10*, 861–864.

Clifford, D.M., Wolfe, B.A., Roberts-Galbraith, R.H., McDonald, W.H., Yates, J.R., 3rd, and Gould, K.L. (2008). The Clp1/Cdc14 phosphatase contributes to the robustness of cytokinesis by association with anillin-related Mid1. J. Cell Biol. *181*, 79–88.

Cohen-Fix, O., Peters, J.M., Kirschner, M.W., and Koshland, D. (1996). Anaphase initiation in Saccharomyces cerevisiae is controlled by the APC-dependent degradation of the anaphase inhibitor Pds1p. Genes Dev. *10*, 3081–3093.

Collin, P., Nashchekina, O., Walker, R., and Pines, J. (2013). The spindle assembly checkpoint works like a rheostat rather than a toggle switch. Nat. Cell Biol. *15*, 1378–1385.

Cornu, M., Albert, V., and Hall, M.N. (2013). mTOR in aging, metabolism, and cancer. Curr. Opin. Genet. Dev. *23*.

Cuyàs, E., Corominas-Faja, B., Joven, J., and Menendez, J.A. (2014). Cell cycle regulation by the nutrient-sensing mammalian target of rapamycin (mTOR) pathway. Methods Mol. Biol. *1170*, 113–144.

D'Amours, D., and Amon, A. (2004). At the interface between signaling and executing anaphase–Cdc14 and the FEAR network. Genes Dev. *18*, 2581–2595.

Daicho, K., Koike, N., Ott, R.G., Daum, G., and Ushimaru, T. (2020). TORC1 ensures membrane trafficking of Tat2 tryptophan permease via a novel transcriptional activator Vhr2 in budding yeast. Cell Signal *68*, 109542.

Diaz-Cuervo, H., and Bueno, A. (2008). Cds1 controls the release of Cdc14-like phosphatase Flp1 from the nucleolus to drive full activation of the checkpoint response to replication stress in fission yeast. Mol. Biol. Cell *19*, 2488–2499.

Dick, A.E., and Gerlich, D.W. (2013). Kinetic framework of spindle assembly checkpoint signalling. Nat. Cell Biol. *15*, 1370–1377.

Dryden, S.C., Nahhas, F.A., Nowak, J.E., Goustin, A.S., and Tainsky, M.A. (2003). Role for human SIRT2 NAD-dependent deacetylase activity in control of mitotic exit in the cell cycle. Mol. Cell Biol. *23*, 3173–3185.

Eguren, M., Porlan, E., Manchado, E., García-Higuera, I., Cañamero, M., Fariñas, I., and Malumbres, M. (2013). The APC/C cofactor Cdh1 prevents replicative stress and p53-dependent cell death in neural progenitors. Nat. Commun. *4*, 2880.

Esteban, V., Blanco, M., Cueille, N., Simanis, V., Moreno, S., and Bueno, A. (2004). A role for the Cdc14-family phosphatase Flp1p at the end of the cell cycle in controlling the rapid degradation of the mitotic inducer Cdc25p in fission yeast. J. Cell Sci. *117*, 2461–2468.

Fingar, D.C., Richardson, C.J., Tee, A.R., Cheatham, L., Tsou, C., and Blenis, J. (2004). mTOR controls cell cycle progression through its cell growth effectors S6K1 and 4E-BP1/eukaryotic translation initiation factor 4E. Mol. Cell Biol. *24*, 200–216.

Gascoigne, K.E., and Taylor, S.S. (2008). Cancer cells display profound intra- and interline variation following prolonged exposure to antimitotic drugs. Cancer Cell *14*, 111–122.

Gavin, A.C., Aloy, P., Grandi, P., Krause, R., Boesche, M., Marzioch, M., Rau, C., Jensen, L.J., Bastuck, S., Dumpelfeld, B., et al. (2006). Proteome survey reveals modularity of the yeast cell machinery. Nature *440*, 631–636.

Gelperin, D.M., White, M.A., Wilkinson, M.L., Kon, Y., Kung, L.A., Wise, K.J., Lopez-Hoyo, N., Jiang, L., Piccirillo, S., Yu, H., et al. (2005). Biochemical and genetic analysis of the yeast proteome with a movable ORF collection. Genes Dev. *19*, 2816–2826.

Goldstein, A.L., and McCusker, J.H. (1999). Three new dominant drug resistance cassettes for gene disruption in *Saccharomyces cerevisiae*. Yeast *15*, 1541–1553.

Grallert, A., Boke, E., Hagting, A., Hodgson, B., Connolly, Y., Griffiths, J.R., Smith, D.L., Pines, J., and Hagan, I.M. (2015). A PP1-PP2A phosphatase relay controls mitotic progression. Nature *517*, 94–98.

Hagting, A., Den Elzen, N., Vodermaier, H.C., Waizenegger, I.C., Peters, J.M., and Pines, J. (2002). Human securin proteolysis is controlled by the spindle checkpoint and reveals when the APC/C switches from activation by Cdc20 to Cdh1. J. Cell Biol. *157*, 1125–1137.

Hardwick, K.G., Weiss, E., Luca, F.C., Winey, M., and Murray, A.W. (1996). Activation of the budding yeast spindle assembly checkpoint without mitotic spindle disruption. Science *273*, 953–956.

Huang, H.C., Mitchison, T.J., and Shi, J. (2010). Stochastic competition between mechanistically independent slippage and death pathways determines cell fate during mitotic arrest. PLoS One *5*, e15724.

Huang, H.C., Shi, J., Orth, J.D., and Mitchison, T.J. (2009). Evidence that mitotic exit is a better cancer therapeutic target than spindle assembly. Cancer Cell *16*, 347–358.

Huh, W.K., Falvo, J.V., Gerke, L.C., Carroll, A.S., Howson, R.W., Weissman, J.S., and O'Shea, E.K. (2003). Global analysis of protein localization in budding yeast. Nature *425*, 686–691.

Jaspersen, S.L., Charles, J.F., and Morgan, D.O. (1999). Inhibitory phosphorylation of the APC regulator Hct1 is controlled by the kinase Cdc28 and the phosphatase Cdc14. Curr. Biol. *9*, 227–236.

Jeganathan, K.B., Malureanu, L., and van Deursen, J.M. (2005). The Rae1-Nup98 complex prevents aneuploidy by inhibiting securin degradation. Nature *438*, 1036–1039.

Jiang, Y., and Broach, J.R. (1999). Tor proteins and protein phosphatase 2A reciprocally regulate Tap42 in controlling cell growth in yeast. EMBO J. *18*, 2782–2792.

Kaiser, B.K., Zimmerman, Z.A., Charbonneau, H., and Jackson, P.K. (2002). Disruption of centrosome structure, chromosome segregation, and cytokinesis by misexpression of human Cdc14A phosphatase. Mol. Biol. Cell *13*, 2289–2300.

Kidokoro, T., Tanikawa, C., Furukawa, Y., Katagiri, T., Nakamura, Y., and Matsuda, K. (2008). CDC20, a potential cancer therapeutic target, is negatively regulated by p53. Oncogene *27*, 1562–1571.

Kondo, A., Mostofa, M.G., Miyake, K., Terasawa, M., Nafisa, I., Yeasmin, A., Waliullah, T.M., Kanki, T., and Ushimaru, T. (2018). Cdc14 phosphatase promotes TORC1-regulated autophagy in yeast. J. Mol. Biol. *430*, 1671–1684.

Kulukian, A., Han, J.S., and Cleveland, D.W. (2009). Unattached kinetochores catalyze production of an anaphase inhibitor that requires a Mad2 template to prime Cdc20 for BubR1 binding. Dev. Cell *16*, 105–117.

Kushnirov, V.V. (2000). Rapid and reliable protein extraction from yeast. Yeast *16*, 857–860.

Lauze, E., Stoelcker, B., Luca, F.C., Weiss, E., Schutz, A.R., and Winey, M. (1995). Yeast spindle pole body duplication gene MPS1 encodes an essential dual specificity protein kinase. EMBO J. *14*, 1655–1663.

Lee, J., Kim, J.A., Margolis, R.L., and Fotedar, R. (2010). Substrate degradation by the anaphase promoting complex occurs during mitotic slippage. Cell Cycle *9*, 1792–1801.

Liu, W., Li, W., Fujita, T., Yang, Q., and Wan, Y. (2008). Proteolysis of CDH1 enhances susceptibility to UV radiation-induced apoptosis. Carcinogenesis *29*, 263–272.

Loewith, R., and Hall, M.N. (2011). Target of Rapamycin (TOR) in nutrient signaling and growth control. Genetics *189*, 1177–1201.

Manchado, E., Eguren, M., and Malumbres, M. (2010). The anaphase-promoting complex/cyclosome (APC/C): cell-cycle-dependent and -independent functions. Biochem. Soc. Trans. *38*, 65–71.

Matsui, A., Kamada, Y., and Matsuura, A. (2013). The role of autophagy in genome stability through suppression of abnormal mitosis under starvation. PLoS Genet. *9*, e1003245.

Michaelis, C., Ciosk, R., and Nasmyth, K. (1997). Cohesins: chromosomal proteins that prevent premature separation of sister chromatids. Cell *91*, 35–45.

Minn, A.J., Boise, L.H., and Thompson, C.B. (1996). Expression of Bcl-xL and loss of p53 can cooperate to overcome a cell cycle checkpoint induced by mitotic spindle damage. Genes Dev. *10*, 2621–2631.

Mocciaro, A., Berdougo, E., Zeng, K., Black, E., Vagnarelli, P., Earnshaw, W., Gillespie, D., Jallepalli, P., and Schiebel, E. (2010). Vertebrate cells genetically deficient for Cdc14A or Cdc14B retain DNA damage checkpoint proficiency but are impaired in DNA repair. J. Cell Biol. *189*, 631–639.

Mochida, S., Ikeo, S., Gannon, J., and Hunt, T. (2009). Regulated activity of PP2A-B55 delta is crucial for controlling entry into and exit from mitosis in Xenopus egg extracts. EMBO J. *28*, 2777–2785.

Mostofa, M.G., Morshed, S., Mase, S., Hosoyamada, S., Kobayashi, T., and Ushimaru, T. (2021). Cdc14 protein phosphatase and topoisomerase II mediate rDNA dynamics and nucleophagic degradation of nucleolar proteins after TORC1 inactivation. Cell Signal *79*, 109884.

Musacchio, A., and Salmon, E.D. (2007). The spindle-assembly checkpoint in space and time. Nat. Rev. Mol. Cell Biol. *8*, 379–393.

Nagai, M., and Ushimaru, T. (2014). Cdh1 is an antagonist of the spindle assembly checkpoint. Cell Signal *26*, 2217–2222.

Nakashima, A., Maruki, Y., Imamura, Y., Kondo, C., Kawamata, T., Kawanishi, I., Takata, H., Matsuura, A., Lee, K.S., Kikkawa, U., et al. (2008). The yeast Tor signaling pathway is involved in G2/M transition via polo-kinase. PLoS One *3*, e2223.

Nishimura, K., Fukagawa, T., Takisawa, H., Kakimoto, T., and Kanemaki, M. (2009). An auxin-based degron system for the rapid depletion of proteins in nonplant cells. Nat. Methods *6*, 917–922.

Ohkura, H., Kinoshita, N., Miyatani, S., Toda, T., and Yanagida, M. (1989). The fission yeast dis2+ gene required for chromosome disjoining encodes one of two putative type 1 protein phosphatases. Cell *57*, 997–1007.

Peddibhotla, S., Wei, Z., Papineni, R., Lam, M.H., Rosen, J.M., and Zhang, P. (2011). The DNA damage effector Chk1 kinase regulates Cdc14B nucleolar shuttling during cell cycle progression. Cell Cycle *10*, 671–679.

Peters, J.M., Tedeschi, A., and Schmitz, J. (2008). The cohesin complex and its roles in chromosome biology. Genes Dev. *22*, 3089–3114.

Pines, J. (2006). Mitosis: a matter of getting rid of the right protein at the right time. Trends Cell Biol. *16*, 55–63.

Platani, M., Samejima, I., Samejima, K., Kanemaki, M.T., and Earnshaw, W.C. (2018). Seh1 targets GATOR2 and Nup153 to mitotic chromosomes. J. Cell Sci. *131*, jcs213140.

Qiao, X., Zhang, L., Gamper, A.M., Fujita, T., and Wan, Y. (2010). APC/C-Cdh1: from cell cycle to cellular differentiation and genomic integrity. Cell Cycle *9*, 3904–3912.

Queralt, E., and Uhlmann, F. (2008). Cdk-counteracting phosphatases unlock mitotic exit. Curr. Opin. Cell Biol. *20*, 661–668.

Quimby, B.B., Arnaoutov, A., and Dasso, M. (2005). Ran GTPase regulates Mad2 localization to the nuclear pore complex. Eukaryot. Cell *4*, 274–280.

Rahman, M.A., Mostofa, M.G., and Ushimaru, T. (2018). The Nem1/Spo7-Pah1/lipin axis is required for autophagy induction after TORC1 inactivation. FEBS J. *285*, 1840–1860.

Ramírez-Valle, F., Badura, M.L., Braunstein, S., Narasimhan, M., and Schneider, R.J. (2010). Mitotic raptor promotes mTORC1 activity, G(2)/M cell cycle progression, and internal ribosome entry site-mediated mRNA translation. Mol. Cell Biol. *30*, 3151–3164.

Rieder, C.L., and Maiato, H. (2004). Stuck in division or passing through: what happens when cells cannot satisfy the spindle assembly checkpoint. Dev. Cell *7*, 637–651.

Rodier, G., Coulombe, P., Tanguay, P.L., Boutonnet, C., and Meloche, S. (2008). Phosphorylation of Skp2 regulated by CDK2 and Cdc14B protects it from degradation by APC(Cdh1) in G1 phase. EMBO J. *27*, 679–691.

Ross, K.E., and Cohen-Fix, O. (2003). The role of Cdh1p in maintaining genomic stability in budding yeast. Genetics *165*, 489–503.

Schmitz, M.H., Held, M., Janssens, V., Hutchins, J.R., Hudecz, O., Ivanova, E., Goris, J., Trinkle-Mulcahy, L., Lamond, A.I., Poser, I., et al. (2010). Live-cell imaging RNAi screen identifies PP2A-B55alpha and importin-beta1 as key mitotic exit regulators in human cells. Nat. Cell Biol. *12*, 886–893.

Schwab, M., Lutum, A.S., and Seufert, W. (1997). Yeast Hct1 is a regulator of Clb2 cyclin proteolysis. Cell *90*, 683–693.

Severin, F., Hyman, A.A., and Piatti, S. (2001). Correct spindle elongation at the metaphase/anaphase transition is an APC-dependent event in budding yeast. J. Cell Biol. *155*, 711–718.

Shimobayashi, M., and Hall, M.N. (2014). Making new contacts: the mTOR network in metabolism and signalling crosstalk. Nat. Rev. Mol. Cell Biol. *15*, 155–162.

Shirayama, M., Toth, A., Galova, M., and Nasmyth, K. (1999). APC(Cdc20) promotes exit from mitosis by destroying the anaphase inhibitor Pds1 and cyclin Clb5. Nature *402*, 203–207.

Shou, W., Azzam, R., Chen, S.L., Huddleston, M.J., Baskerville, C., Charbonneau, H., Annan, R.S., Carr, S.A., and Deshaies, R.J. (2002). Cdc5 influences phosphorylation of Net1 and disassembly of the RENT complex. BMC Mol. Biol. *3*, 3.

Shou, W., and Deshaies, R.J. (2002). Multiple telophase arrest bypassed (tab) mutants alleviate the essential requirement for Cdc15 in exit from mitosis in S. cerevisiae. BMC Genet. *3*, 4.

Shou, W., Seol, J.H., Shevchenko, A., Baskerville, C., Moazed, D., Chen, Z.W., Jang, J., Shevchenko, A., Charbonneau, H., and Deshaies, R.J. (1999). Exit from mitosis is triggered by Tem1-dependent release of the protein phosphatase Cdc14 from nucleolar RENT complex. Cell *97*, 233–244.

Simanis, V. (2003). Events at the end of mitosis in the budding and fission yeasts. J. Cell Sci. *116*, 4263–4275.

Stegmeier, F., and Amon, A. (2004). Closing mitosis: the functions of the Cdc14 phosphatase and its regulation. Annu. Rev. Genet. *38*, 203–232.

Stegmeier, F., Visintin, R., and Amon, A. (2002). Separase, polo kinase, the kinetochore protein Slk19, and Spo12 function in a network that controls Cdc14 localization during early anaphase. Cell *108*, 207–220.

Straight, A.F., Sedat, J.W., and Murray, A.W. (1998). Time-lapse microscopy reveals unique roles for kinesins during anaphase in budding yeast. J. Cell Biol. *143*, 687–694.

Straight, A.F., Shou, W., Dowd, G.J., Turck, C.W., Deshaies, R.J., Johnson, A.D., and Moazed, D. (1999). Net1, a Sir2-associated nucleolar protein required for rDNA silencing and nucleolar integrity. Cell *97*, 245–256.

Sudo, T., Ota, Y., Kotani, S., Nakao, M., Takami, Y., Takeda, S., and Saya, H. (2001). Activation of Cdh1-dependent APC is required for G1 cell cycle arrest and DNA damage-induced G2 checkpoint in vertebrate cells. EMBO J. *20*, 6499–6508.

Sullivan, M., and Morgan, D.O. (2007). Finishing mitosis, one step at a time. Nat. Rev. Mol. Cell Biol. *8*, 894–903.

Tan, A.L., Rida, P.C., and Surana, U. (2005). Essential tension and constructive destruction: the spindle checkpoint and its regulatory links with mitotic exit. Biochem. J. *386*, 1–13.

Toda, K., Naito, K., Mase, S., Ueno, M., Uritani, M., Yamamoto, A., and Ushimaru, T. (2012). APC/C-Cdh1-dependent anaphase and telophase progression during mitotic slippage. Cell Div. *7*, 4.

Topham, C.H., and Taylor, S.S. (2013). Mitosis and apoptosis: how is the balance set? Curr. Opin. Cell Biol. *25*, 780–785.

Tran, L.T., Wang'ondu, R.W., Weng, J.B., Wanjiku, G.W., Fong, C.M., Kile, A.C., Koepp, D.M., and Hood-Degrenier, J.K. (2010). TORC1 kinase and the S-phase cyclin Clb5 collaborate to

promote mitotic spindle assembly and DNA replication in S. cerevisiae. Curr. Genet. *2010*, 10.

van Leuken, R., Clijsters, L., and Wolthuis, R. (2008). To cell cycle, swing the APC/C. Biochim. Biophys. Acta *1786*, 49–59.

Vignot, S., Faivre, S., Aguirre, D., and Raymond, E. (2005). mTOR-targeted therapy of cancer with rapamycin derivatives. Ann. Oncol. *16*, 525–537.

Visintin, R., Craig, K., Hwang, E.S., Prinz, S., Tyers, M., and Amon, A. (1998). The phosphatase Cdc14 triggers mitotic exit by reversal of Cdk-dependent phosphorylation. Mol. Cell *2*, 709–718.

Visintin, R., Hwang, E.S., and Amon, A. (1999). Cfi1 prevents premature exit from mitosis by anchoring Cdc14 phosphatase in the nucleolus. Nature *398*, 818–823.

Visintin, R., Prinz, S., and Amon, A. (1997). CDC20 and CDH1: a family of substrate-specific activators of APC-dependent proteolysis. Science *278*, 460–463.

Warren, C.D., Brady, D.M., Johnston, R.C., Hanna, J.S., Hardwick, K.G., and Spencer, F.A. (2002). Distinct chromosome segregation roles for spindle checkpoint proteins. Mol. Biol. Cell *13*, 3029–3041.

Wasch, R., Robbins, J.A., and Cross, F.R. (2010). The emerging role of APC/CCdh1 in controlling differentiation, genomic stability and tumor suppression. Oncogene *29*, 1–10.

Wolfe, B.A., and Gould, K.L. (2004). Fission yeast Clp1p phosphatase affects G2/M transition and mitotic exit through Cdc25p inactivation. EMBO J. *23*, 919–929.

Wu, J.Q., Guo, J.Y., Tang, W., Yang, C.S., Freel, C.D., Chen, C., Nairn, A.C., and Kornbluth, S. (2009). PP1-mediated dephosphorylation of phosphoproteins at mitotic exit is controlled by inhibitor-1 and PP1 phosphorylation. Nat. Cell Biol. *11*, 644–651.

Yamamoto, K., Makino, N., Nagai, M., Honma, Y., Araki, H., and Ushimaru, T. (2018). TORC1 signaling regulates DNA replication via DNA replication protein levels. Biochem. Biophys. Res. Commun. *505*, 1128–1133.

Yeasmin, A.M., Waliullah, T.M., Kondo, A., Kaneko, A., Koike, N., and Ushimaru, T. (2016). Orchestrated action of PP2A antagonizes Atg13 phosphorylation and promotes autophagy after the inactivation of TORC1. PLoS One *11*, e0166636.

Yoshida, S., Asakawa, K., and Toh-e, A. (2002). Mitotic exit network controls the localization of Cdc14 to the spindle pole body in Saccharomyces cerevisiae. Curr. Biol. *12*, 944–950.

Zinzalla, V., Graziola, M., Mastriani, A., Vanoni, M., and Alberghina, L. (2007). Rapamycin-mediated G1 arrest involves regulation of the Cdk inhibitor Sic1 in Saccharomyces cerevisiae. Mol. Microbiol. *63*, 1482–1494.

Zoncu, R., Efeyan, A., and Sabatini, D.M. (2011). mTOR: from growth signal integration to cancer, diabetes and ageing. Nat. Rev. Mol. Cell Biol. *12*, 21–35.

Zur, A., and Brandeis, M. (2001). Securin degradation is mediated by fzy and fzr, and is required for complete chromatid separation but not for cytokinesis. EMBO J. *20*, 792–801.

STAR★METHODS

KEY RESOURCES TABLE

REAGENT or RESOURCE	SOURCE	IDENTIFIER
Antibodies		
Mouse monoclonal anti-HA (F7)	Santa Cruz	Cat#sc-7392; RRID:AB_2894930
Peroxidase-anti-peroxidase soluble complex (PAP)	Sigma-Aldrich	Cat#P1291; RRID:AB_1079562
Rabbit polyclonal anti-IAA17	Gift from M. Kanemaki	N/A
Mouse monoclonal anti-CDK (PSTAIRE)	Santa Cruz	Cat#sc-53; RRID:AB_2074908
Mouse monoclonal anti-Pgk1	Thermo Fisher Scientific	Cat#A-6457; RRID:AB_221541
Rabbit polyclonal anti-Cdh1	Novus Biologicals	Cat#NBP2-15840; RRID:AB_2895137
Rabbit polyclonal anti-Cdc20	Protein Tech Group	Cat#10252-1-AP; RRID: AB_2229016
Rabbit polyclonal anti-phospho-p70 S6 kinase	Cell Signaling Technology	Cat#9205; RRID:AB_330944
Rabbit polyclonal anti-p70 S6 kinase	Cell Signaling Technology	Cat#9202; RRID:AB_331676
Mouse monoclonal anti-α−tubulin	Sigma	Cat#T6074; RRID:AB_477582
Rabbit polyclonal anti-Mad1	GeneTex	Cat#GTX109519; RRID:AB_1950847
Mouse monoclonal anti-Cyclin B	BD Biosciences	Cat#610219; RRID:AB_397616
Human polyclonal anti-centromere protein antibody	Antibodies Inc.	Cat#15-234; RRID:AB_2687472
Goat polyclonal anti-Mouse IgG Alexa Fluor-488	Thermo Fisher Scientific	Cat#A11029; RRID:AB_138404
Goat polyclonal anti-Rabbit IgG Alexa Fluor-488	Thermo Fisher Scientific	Cat#A11034; RRID:AB_2576217
Goat polyclonal Anti-Human IgG Alexa Fluor-568	Thermo Fisher Scientific	Cat#A21090; RRID:AB_1500627
Bacterial and virus strains		
JM109	Takara	Cat#9052
Chemicals, peptides, and recombinant proteins		
Rapamycin	LC Laboratories	Cat#R5000; CAS:53123-88-9
Nocodazole	Sigma-Aldrich	Cat#M1404; CAS:31430-18-9
4′,6-diamidino-2-phenylindole (DAPI)	Dojin	Cat#D212; CAS:28718-90-3
ProLong Gold	Thermo Fisher Scientific	Cat#P36930
MG132	Sigma-Aldrich	Cat#474790; CAS:133407-82-6
Femtoglow Plus	Michigan Diagnostics	Cat# 21008
ECL prime Western Blotting Detection Reagents	Cytiva	Cat#GERPN2236
Western BLoT Quant HRP Substrate	Takara	Cat#T7102
RNase A	Nippon Gene	Cat#318-06391
Experimental models: Cell lines		
Human: A549	ATCC Cell Bank	Cat#CCL-185; RRID:CVCL_0023
Experimental models: Organisms/strains		
S. cerevisiae: *MATa his3-11,15 trp1-1 leu2-3,112 ura3-1 ade2-1 can1-1*	Lab stock	W303a
S. cerevisiae: W303a *bar1::hisG*	Lab stock	SCU893 (US356)
S. cerevisiae: *MATα gal2*	Lab stock	S288C

(*Continued on next page*)

Continued

REAGENT or RESOURCE	SOURCE	IDENTIFIER
S. cerevisiae: S288C *MATa ade2 arg4 leu2-3,112 trp1-289, ura3-52*	(Gavin et al., 2006)	MGD353-13D
S. cerevisiae: S288C *MATa ura3Δ0 leu2Δ0 his3Δ1 met15Δ0*	Lab stock	BY4741
S. cerevisiae: SCU893 *trp1::LacO::TRP1 his3::LacI-GFP::HIS3*	This study	SCU69
S. cerevisiae: W303a *scc1-73*	(Michaelis et al., 1997)	SCU244
S. cerevisiae: W303a *cdc14::CDC14-5×GFP::TRP1*	Gift from A. Toh-e	SCU1000
S. cerevisiae: W303a *cdc14-1*	Gift from A. Toh-e	SCU1001
S. cerevisiae: W303a *MATα CDC14^{TAB6-1}*	(Shou and Deshaies, 2002)	SCU1199
S. cerevisiae: W303a *cdh1::kanR bar1*	(Ross and Cohen-Fix, 2003)	SCU1228
S. cerevisiae: W303a + CFIII (CEN3.L.YPH278) *URA3 SUP11*	(Warren et al., 2002)	SCU1237
S. cerevisiae: SCU893 *mad2::hphMX* [pMAD2-GFP::URA3]	This study	SCU1337
S. cerevisiae: BY4741 *BUB1-GFP::HIS3MX*	(Huh et al., 2003)	SCU1485
S. cerevisiae: MGD353-13D *CLB5-TAP::KlURA3*	(EUROSCARF) (Gavin et al., 2006)	SCU1712
S. cerevisiae: MGD353-13D *CLB2-TAP::KlURA3*	(EUROSCARF) (Gavin et al., 2006)	SCU1709
S. cerevisiae: MGD353-13D *SCC1-TAP::KlURA3*	(EUROSCARF) (Gavin et al., 2006)	SCU1964
S. cerevisiae: W303a *cdh1::kanR bar1 trp1::LacO::TRP1 his3::LacI-GFP::HIS3*	This study	SCU2114
S. cerevisiae: W303a *cdh1::kanR bar1 ura3::PDS1-HA3::URA3*	This study	SCU2282
S. cerevisiae: SCU893 *PDS1-3HA::URA3 cdc20-3::hphMX*	This study	SCU2693
S. cerevisiae: SCU893 *PDS1-3HA::URA3*	This study	SCU2755
S. cerevisiae: W303a *scc1-73 PDS1-3HA::URA3*	This study	SCU2814
S. cerevisiae: SCU893 *trp1::LacO::TRP1 his3::LacI-GFP::HIS3 cdc14-1::hphMX*	This study	SCU3204
S. cerevisiae: W303a *cdc14-1 PDS1-3HA::URA3*	This study	SCU3250
S. cerevisiae: SCU893 *NET1-HA3::LEU2*	This study	SCU3260
S. cerevisiae: SCU893 *ura3::ADH1pr-osTIR1-9myc::URA3 NET1-IAA17::kanMX*	This study	SCU3331
S. cerevisiae: SCU893 *ura3::ADH1pr-osTIR1-9myc::URA3 NET1-IAA17::kanMX CDC14-5×GFP::TRP1*	This study	SCU3409
S. cerevisiae: SCU893 *atg1::kanMX*	(Rahman et al., 2018)	SCU4067
S. cerevisiae: SCU893 *NET1-IAA17::kanMX ura3::ADH1pr-osTIR1-myc9::URA3 trp1::LacO::TRP1 his3::LacI-GFP::HIS3*	This study	SCU6232
S. cerevisiae: SCU893 *NET1-HA3::LEU2 atg1::kanMX*	This study	SCU6918

(*Continued on next page*)

Continued

REAGENT or RESOURCE	SOURCE	IDENTIFIER
S. cerevisiae: SCU893 *NET1-HA3::LEU2 pdr5::kanMX*	This study	SCU6922
S. cerevisiae: SCU893 *NET1-HA3::LEU2*	This study	SCU7048
S. cerevisiae: SCU893 *ura3::ADH1pr-osTIR1-9myc::URA3 NET1-IAA17::kanMX CDC14-5×GFP::TRP1*	This study	SCU7053
Oligonucleotides		
siRNA targeting sequence:		
Cdh1: UGAGAAGUCUCCCAGUCAGTT	J-Bios	(Brummelkamp et al., 2002)
Cdc20: GGAGCUCAUCUCAGGCCAUTT	J-Bios	(Kidokoro et al., 2008)
Recombinant DNA		
Plasmid: [PCR template] *hphMX4*	(Goldstein and McCusker, 1999)	pSCU452
Plasmid: [YIp] *NET1-HA3 LEU2*	(Straight et al., 1999)	pSCU478
Plasmid: [YIp] *lacO×256 TRP1*	(Straight et al., 1998)	pSCU562
Plasmid: [YIp] *HIS3p-GFP13-LacI12NLS HIS3*	(Straight et al., 1998)	pSCU566
Plasmid: [YIp] *CDC14-5×GFP TRP1*	(Yoshida et al., 2002)	pSCU577
Plasmid: [YIp] *PDS1-HA3 URA3*	(Cohen-Fix et al., 1996)	pSCU784
Plasmid: [YEp] *GAL1p-GST-MPS1 URA3 leu2-d*	(Lauze et al., 1995)	pSCU887
Plasmid: [YCp] *MAD2-GFP URA3*	(Quimby et al., 2005)	pSCU973
Plasmid: [PCR template] *IAA17 KanMX*	(Nishimura et al., 2009)	pSCU1374
Plasmid: [YIp] *ADH1p-osTIR1-9myc URA3*	(Nishimura et al., 2009)	pSCU1413
Plasmid: [YCp] *MTW1-DsRed.T4 LEU2*	This study	pSCU1701
Plasmid: [YEp] *GAL1-NET1-H6HAZZ URA3*	(Gelperin et al., 2005)	pSCU1819
Plasmid: [YCp] *HEH2-RFP LEU2*	(Daicho et al., 2020)	pSCU2196
Plasmid: [YCp] *IFA38-mCherry LEU2*	This study	pSCU2616
Software and algorithms		
DeltaVision softWoRx	Cytiva	https://www.cytivalifesciences.com
CytExpert software	Beckman Coulter	https://www.beckman.com
GraphPad Prism (v. 9.1.1)	GraphPad	https://www.graphpad.com/
Axio Vision	Zeiss	https://www.zeiss.com/
ZEN	Zeiss	https://www.zeiss.com/

RESOURCE AVAILABILITY

Lead contact

Further information and requests for resources and reagents should be directed to and will be fulfilled by the lead contact, Takashi Ushimaru (ushimaru.takashi@shizuoka.ac.jp).

Materials availability

All unique materials generated in this study are available from the Lead Contact with a completed Material Transfer Agreement.

Data and code availability

This study did not generate datasets.

EXPERIMENTAL MODEL AND SUBJECT DETAILS

All *S. cerevisiae* strains used in this study were derived from the W303a (*MATa his3-11,15 trp1-1 leu2-3,112 ura3-1 ade2-1 can1-1*).and S288C (*MATα gal2*) background strains. Human cell line A549 was used.

METHOD DETAILS

Yeast strains, plasmids, and media

S. cerevisiae strains and plasmids used are listed in the KEY RESOURCES TABLE. Gene disruption and tagging were conducted using a conventional one-step PCR-mediated method. Glucose-based YPAD (YPD containing 0.01% adenine) and synthetic minimal medium (SD) complemented with the appropriate nutrients for plasmid maintenance were prepared in a standard manner. SRGly was identical to SD except that it contained 2% raffinose and 3% glycerol instead of 2% glucose. For nitrogen depletion, exponentially growing cells cultured in SD medium were transferred to SD medium without ammonium sulphate or amino acids. For cell cycle arrest in metaphase, nocodazole (10 μg/mL) was added to the cell culture for 3 h.

Western blotting analysis

Proteins were extracted using a post-alkaline extraction method in accordance with the method of Kushnirov (Kushnirov, 2000). Briefly, exponentially growing cells (10 mL culture, OD_{600} = 0.3–0.8) were treated with 200 μL of 0.1 M NaOH for 5 min, and then the cell pellet was collected by centrifugation. The cell pellet was treated with sample buffer (60 mM Tris-HCl (pH 6.8), 5% glycerol, 2% SDS, 4% 2-mercaptoethanol and 0.0025% bromophenol blue) at 95°C for 5 min. Crude extracts were cleared by centrifugation, and the supernatant was subjected to western blotting with specific antibodies for analysis. Chemiluminescence signals for horseradish peroxidase (HRP) were detected using an image analyzer (LAS3000mini or LAS4000-mini, Fuji, Tokyo, Japan). All western blotting experiments were done independently at least twice to confirm the reproducibility of the results.

To check the efficiency of RNAi in human cells, cells were lysed in TNE-N buffer (1% NP-40, 100 mM NaCl, 10 mM Tris-HCl, pH 7.5, and 1 mM EDTA), and were boiled for 10 min with 4×NuPAGE LDS sample buffer (Thermo Fisher Scientific). Proteins in cell lysate were separated using the NuPAGE SDS gel system (Thermo Fisher Scientific) and subjected to western blotting with specific antibodies for analysis.

Microscopic assay of yeast cells

Exponentially growing cells and rapamycin- or nitrogen starvation-treated cells were used for experiments. Cell, GFP, RFP, mCherry, and 4′,6-diamidino-2-phenylindole (DAPI) images were captured using a Carl Zeiss Axio Imager M1 microscope with a cooled CCD camera (Carl Zeiss AxioCam MRm) or a Carl Zeiss Axio Observer 7 microscope with a cooled CCD camera (Carl Zeiss AxioCam 705mono). For DAPI staining, cells were fixed with 70% ethanol briefly, washed with distilled water, and stained with 1 μg/mL DAPI briefly followed by washing. For observations of Mad1-GFP, Bub1-GFP, and Mtw1-RFP the cells were not fixed, because the GFP signals were weak. For statistical analyses, more than 100 cells were counted in each experiment. All experiments were performed at least twice independently to confirm the reproducibility of the results. Data are shown as means ± errors (or SD). Statistical analyses were carried out with the software GraphPad Prism (v. 9.1.1) followed by the two-tailed Fisher's exact test or the two-way ANOVA with Bonferroni correction.

Chromosome instability (CIN) assay

This assay was performed as described previously (Warren et al., 2002). Briefly, strains containing a nonessential *SUP11*-marked mini-chromosome grown in selective media (SD-Ura) were treated with rapamycin (200 ng/mL) and/or nocodazole (10 μg/mL) for 1 h and then were plated at a density of 200 colonies per plate on medium including uracil (SD + Ura). Cells that had lost their mini-chromosomes turn red. Limiting adenine supplementation was used to facilitate red pigment development in *ade2* cells. White colonies with red sectors among more than 100 cells were counted. All experiments were performed at least twice independently. Data are shown as means ± errors. Statistical analyses were carried out using the two-tailed Fisher's exact test.

G1 cell proportion

Nocodazole-treated metaphase cells were treated with 200 ng/mL rapamycin for 4 h. More than 100 cells were examined for each sample, and the proportion of unbudded G1 cells to total cells was calculated. For flow cytometric analysis, cells were prepared according to the manufacturer's instructions. Briefly, yeast cells (1 OD unit) grown in YPAD medium at 30°C until early log phase were treated with rapamycin or nitrogen starvation. Harvested cells were fixed in 70% ethanol, treated with 50 μg/mL RNase A at 50°C for 2 h, sonicated at amplitude 10 for 20 s using an Ultrasonic Processor S4000 (Misonix, Farmingdale, NY),

and stained with 2 μg/mL propidium iodide. DNA contents of propidium iodide-stained cells were analyzed using a CytoFLEX (Beckman Coulter) in accordance with the manufacturer's instructions. Flow cytometric profiles were analyzed by CytExpert software.

Live cell imaging of human cells

A549 cells (ATCC) were grown at 37°C in a 5% CO_2 atmosphere in Dulbecco's modified Eagle's medium (Life Technologies), supplemented with 10% fetal bovine serum and 20 mM HEPES, pH 7.0. For time-lapse imaging, cells were grown in glass chambers (Thermo). Cells were transfected with siRNA using Lipofectamine RNAiMAX reagent (Invitrogen) for 24 h, followed by synchronization with thymidine treatment (2 mM) for 24 h. Then cells were released from the thymidine block in the presence of nocodazole (2 μM). After 12 h, the medium was changed to pre-warmed Leibovitz's L-15 medium (Life Technologies) supplemented with 20% fetal bovine serum and 20 mM HEPES, pH 7.0, in the presence of nocodazole (2 μM) with or without rapamycin (100 nM) and/or MG132 (20 μM). Recordings were made in a temperature-controlled incubator at 37°C. Z-series of three sections in 3 μm increments were captured every 15 min. Image stacks were projected. Images were collected with a BioStudio-T microscope (Nikon) using a ×4 objective lens or ZEISS Celldiscoverer 7 (Zeiss) using a ×20 objective lens. RNA oligonucleotides targeting Cdc20 (Kidokoro et al., 2008) and Cdh1 (Brummelkamp et al., 2002) were used. For control siRNA, Stealth RNAi siRNA negative control med GC duplex #2 (Invitrogen) was used.

Immunofluorescence analysis of human cells

Cells were grown on a glass coverslip and fixed with 3% paraformaldehyde in phosphate buffered saline (PBS; 137 mM NaCl, 2.7 mM KCl, 10 mM Na_2HPO_4, and 1.8 mM KH_2PO_4, pH 7.4) for 10 min at 37°C and permeabilized with 1% Triton X-100 in PBS for 5 min. Fixed cells were incubated for 1 h with the following primary antibodies: anti-Mad1, 1:2000; anti-Cyclin B, 1:2000; and anti-centromere (ACA), 1:2000. The samples were washed with PBS supplemented with 0.02% Triton X-100, and incubated with secondary antibodies coupled with Alexa Fluor–488/568 (1:3,000) for 1 h. Antibody incubations were performed in PBS supplemented with 0.02% Triton X-100. After final washes, cells were mounted with ProLong Gold. Z-image stacks were captured in 0.2-μm increments on an Olympus IX-71 inverted microscope controlled by DeltaVision softWoRx (Cytiva) using ×100 1.40 NA Plan Apochromat oil objective lens (Olympus). Deconvolution was performed when necessary using enhanced ratio algorithm, medium noise filtering, and 10 iterations per channel. Image stacks were projected and saved as Photoshop files.

QUANTIFICATION AND STATISTICAL ANALYSIS

Tests used to determine statistical significance include the two-tailed Fisher's exact test (microscopic analyses in Figures 2D, 2F, 3C–3E and plate assays in Figures 6F and 6G); the two-way ANOVA with Bonferroni correction (microscopic analyses in Figures 5E and 6C); the Tukey's multiple comparison test (microscopic analyses in Figures 7D and 7F); the Dunnett's multiple comparison test (microscopic analyses in Figures S5C and S5E). Statistical Information for each experiment can be found in the figures and corresponding figure legend.